Циклическая вольтамперометрия

Линейная развертка потенциала (potential sweep)

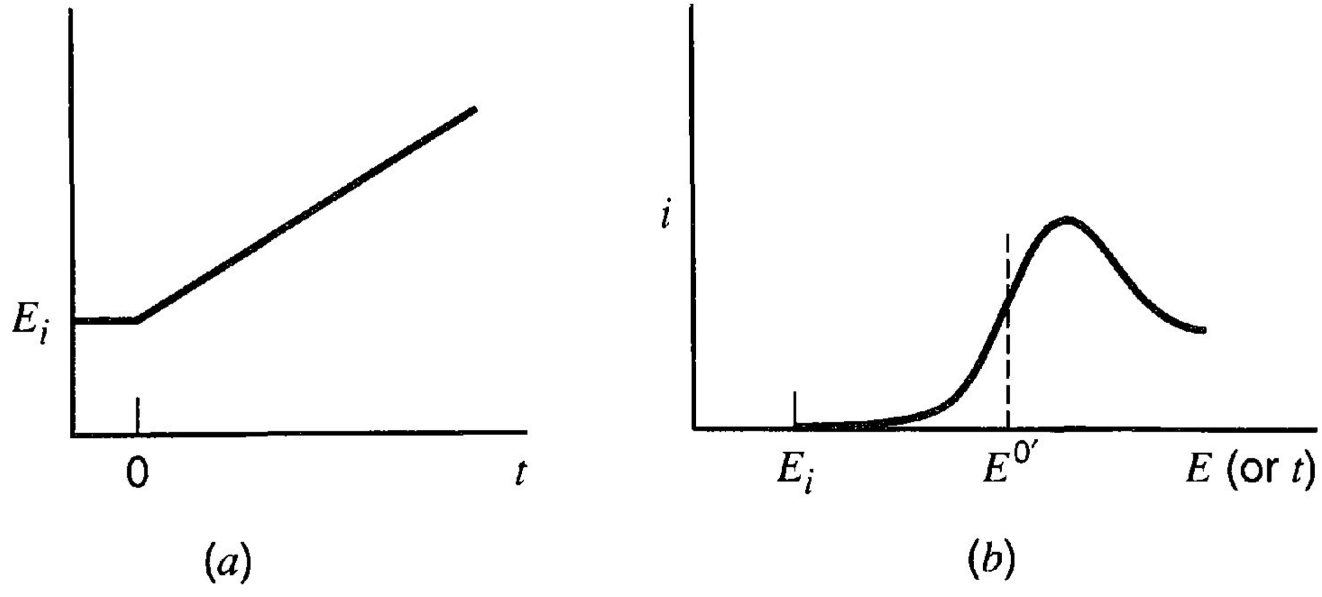

Линейная развертка потенциала (обратимая реакция)

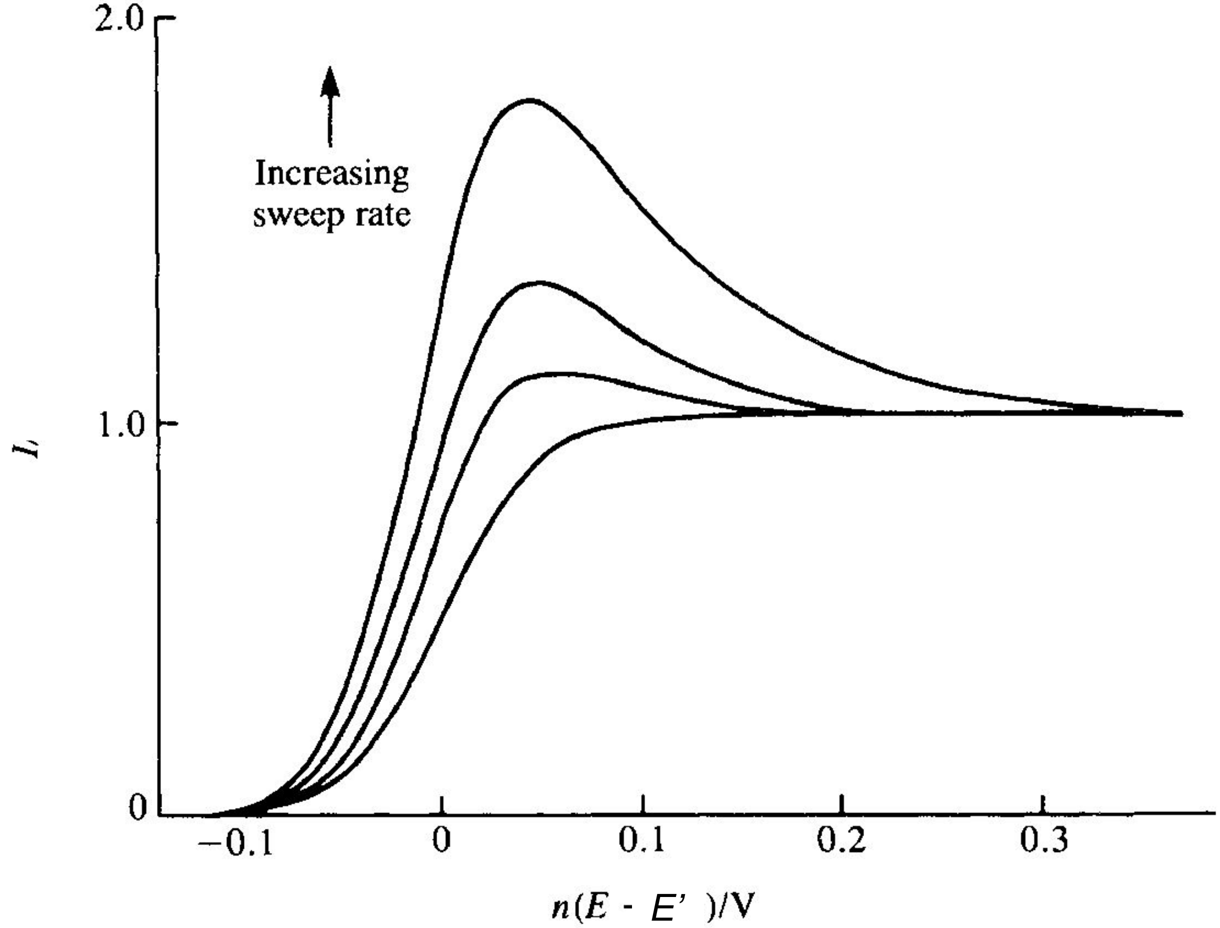

Циклическая вольтамперометрия

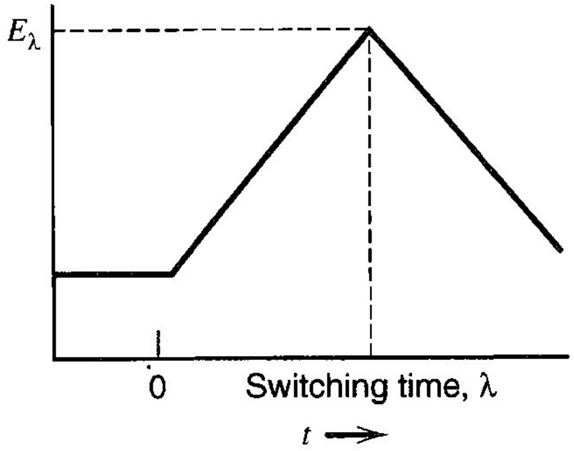

(a)

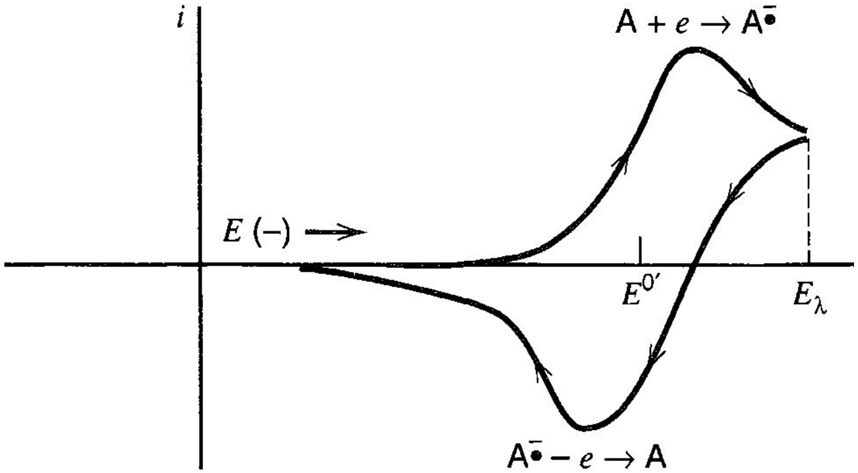

(b)

Циклическая вольтамперометрия

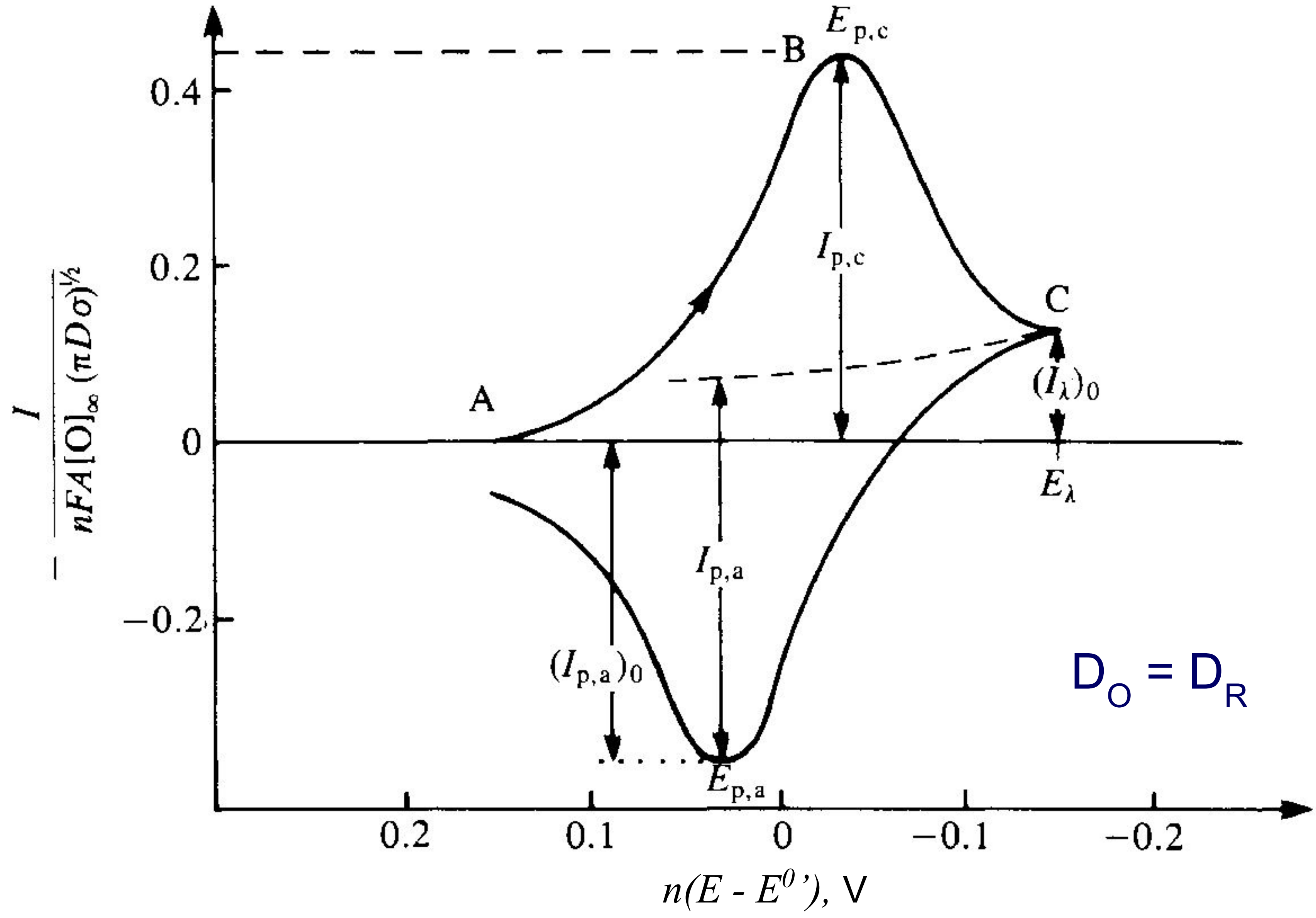

Циклическая вольтамперометрия
обратимая э/х реакция

$$E^{0\prime} = \frac{E_{p,a} + E_{p,c}}{2}$$

$$i_p = 0.4463\frac{(nF)^{3/2}}{\sqrt{RT}} AD^{1/2}C^* v^{1/2}$$

$$\Delta E_p = \frac{59}{n} mV$$

$$i_p \propto v^{1/2}$$

ΔE_p independent of v

$$i_{p,a} = i_{p,c}$$

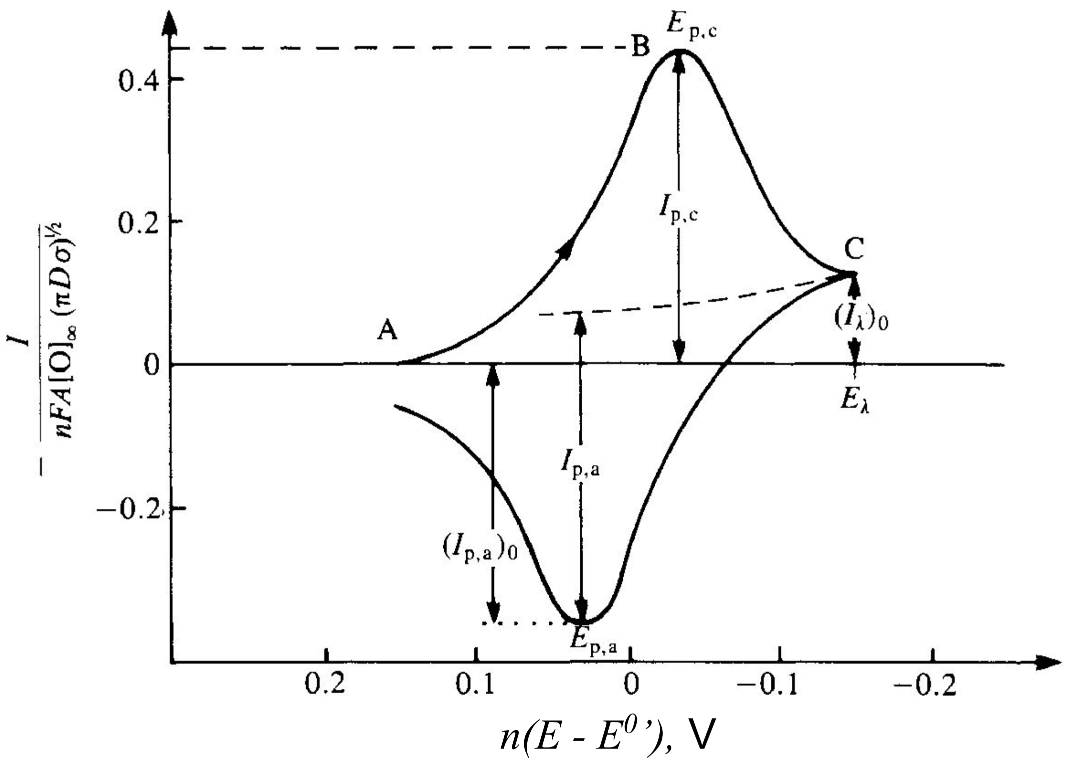

Макро- и микроэлектрод
обратимая э/х реакция

ø = 1.5 mm ø = 10 µm

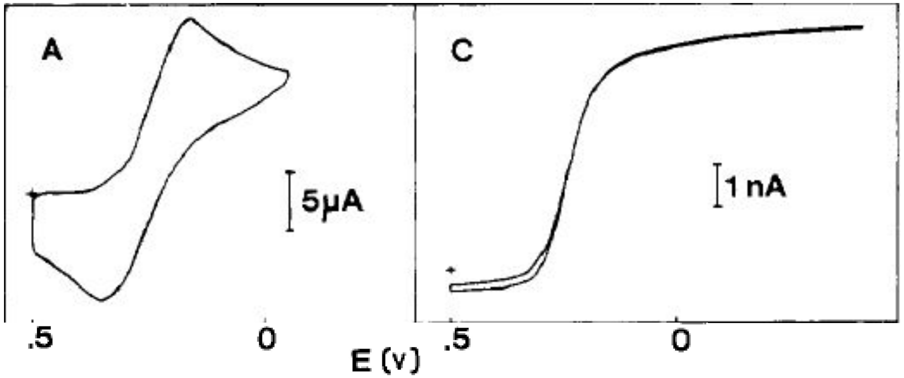

4 mM $K_3[Fe(CN)_6]$ in 0.1 M KCl

100 mV/s

M.A.Dayton, J.C.Brown, K.J.Stutts, R.M.Wightman *Anal. Chem.* **52** (1980) 946-50

Макро- и микроэлектрод
обратимая э/х реакция

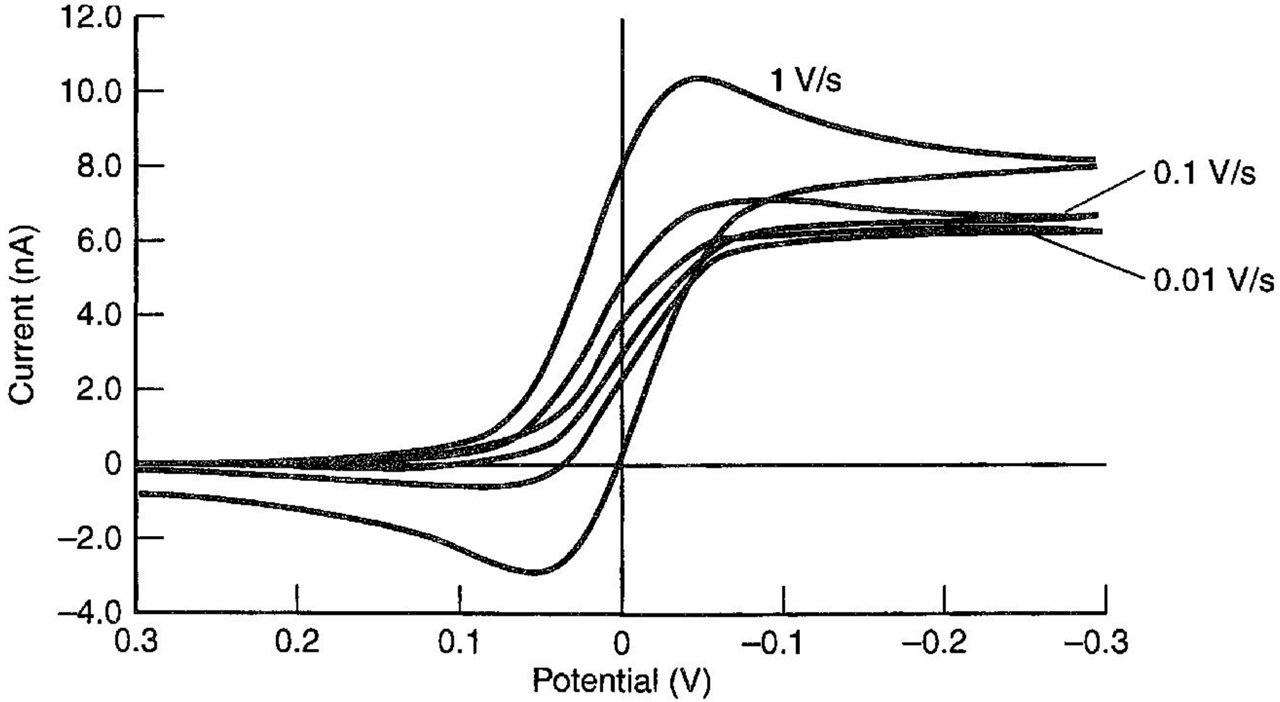

ø = 10 μm

Циклическая вольтамперометрия

влияние емкости

$$|i_c| = AC_d v$$

$$\frac{|i_c|}{i_p} = \frac{C_d v^{1/2}\left(10^{-5}\right)}{2.69 n^{3/2} D^{1/2} C^*}$$

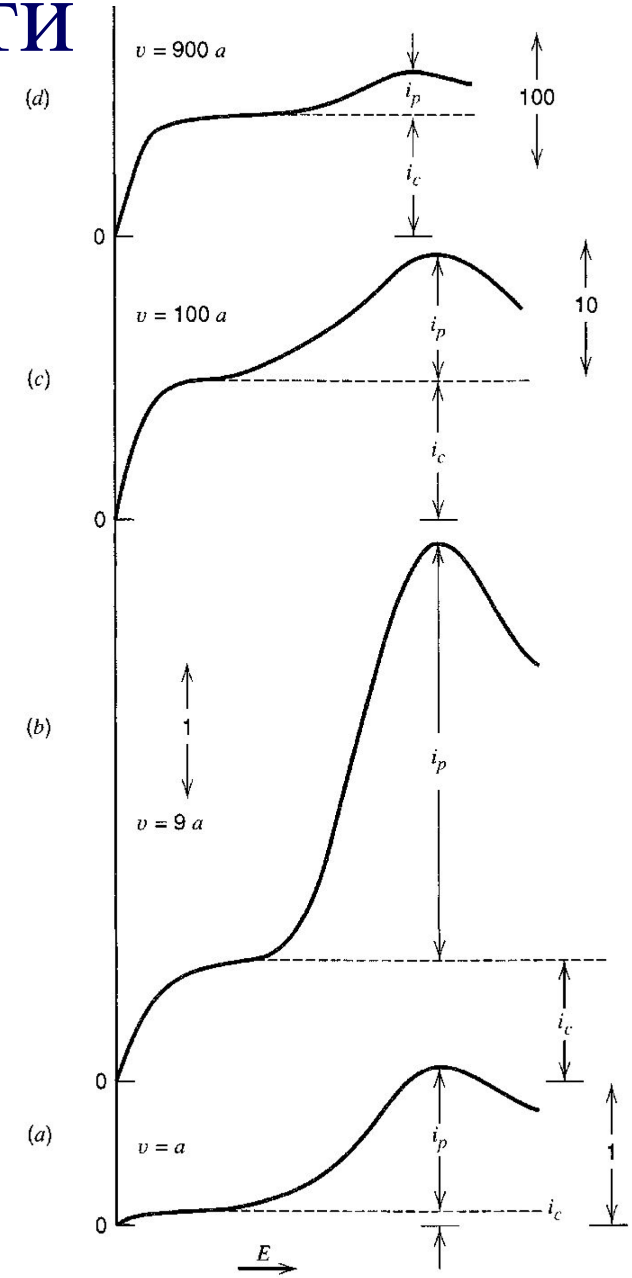

Циклическая вольтамперометрия
необратимая э/х реакция

$$i_p = 0.4958\left(\frac{\alpha F}{RT}\right)^{1/2} FAD^{1/2}C^* v^{1/2}$$

(одноэлектронная)

нет обратного пика

Циклическая вольтамперометрия
квазиобратимая э/х реакция

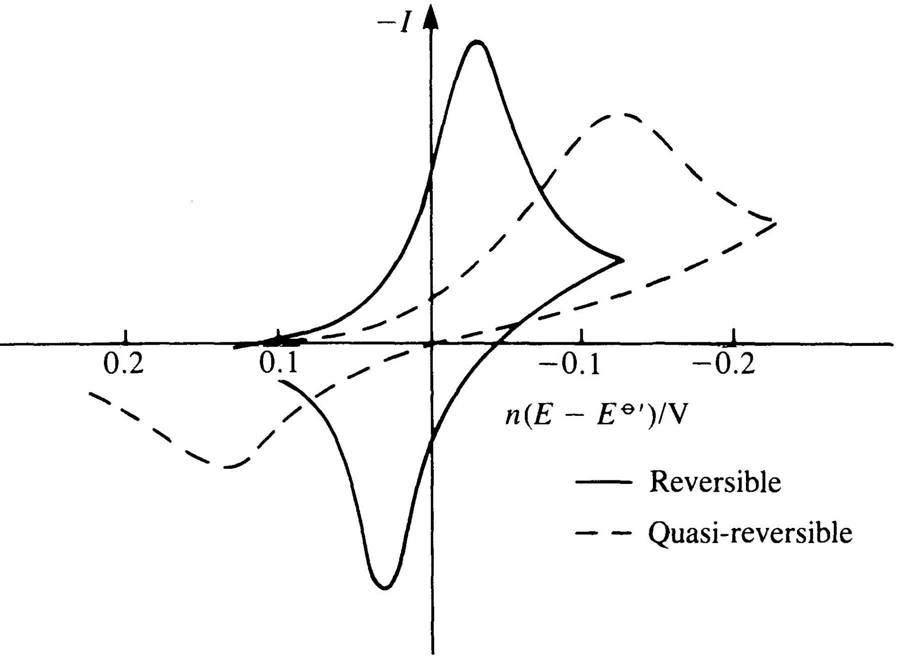

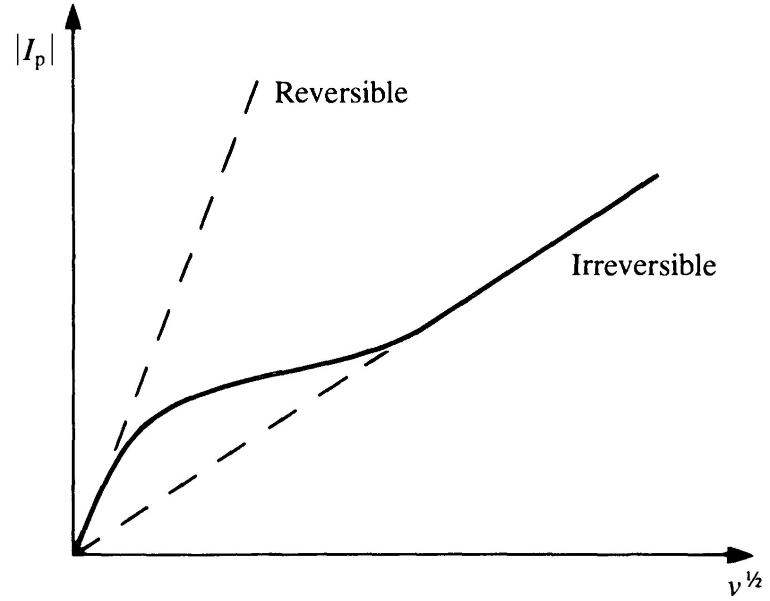

Сопряженная химическая реакция
каталитический механизм

$$O + n\bar{e} \Leftrightarrow R$$

$$R + Z \xrightarrow{k'} O + Y$$

$$i_{\infty} = nFAC_O^* \sqrt{Dk' C_Z^*}$$

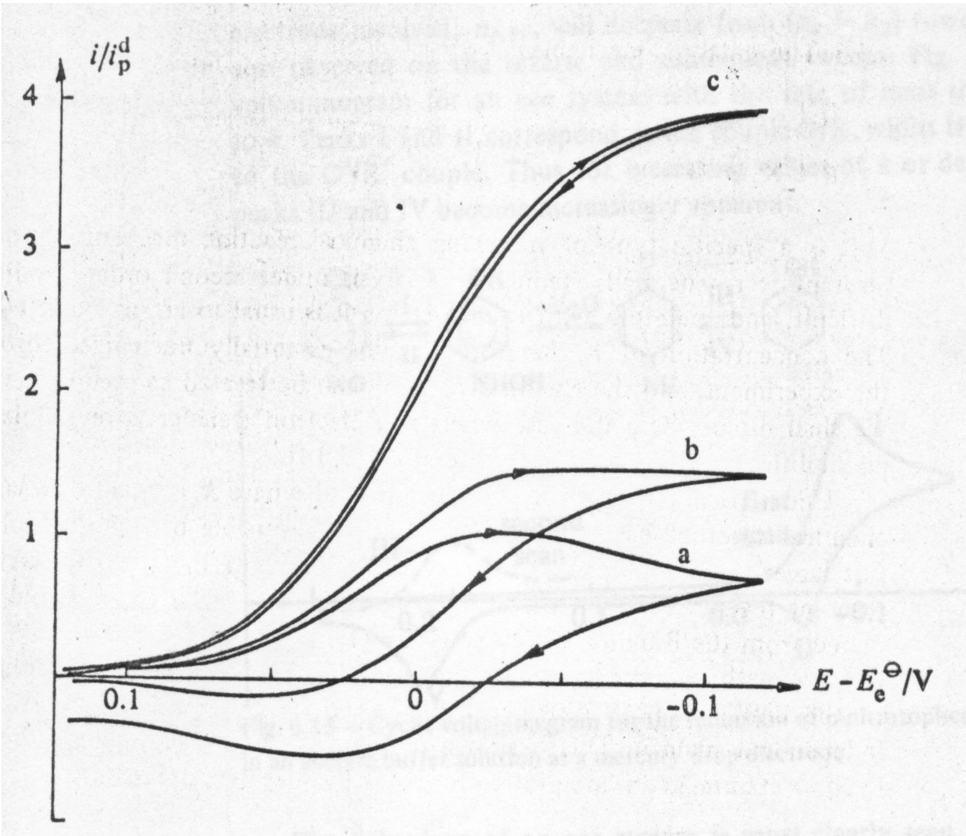

Сопряженная химическая реакция
каталитический механизм

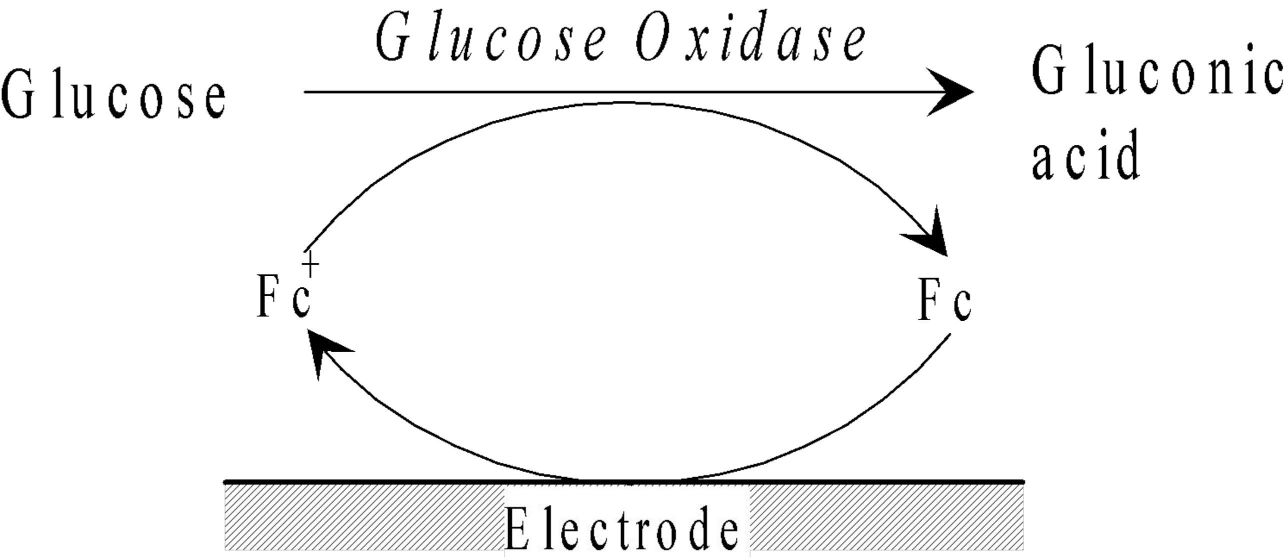

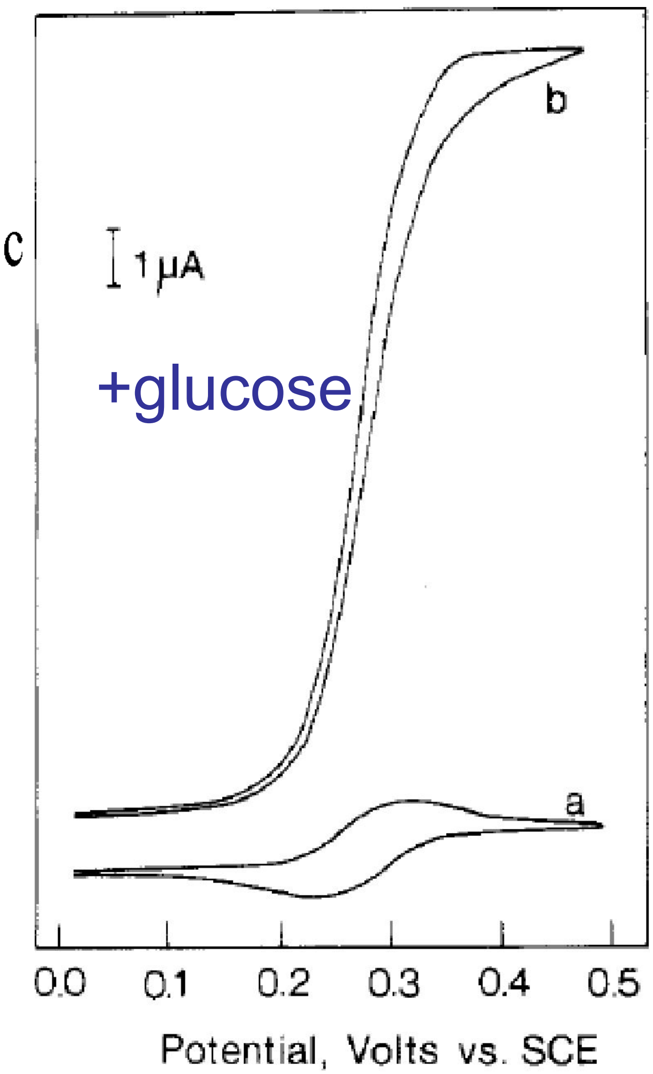

Сопряженная химическая реакция
каталитический механизм

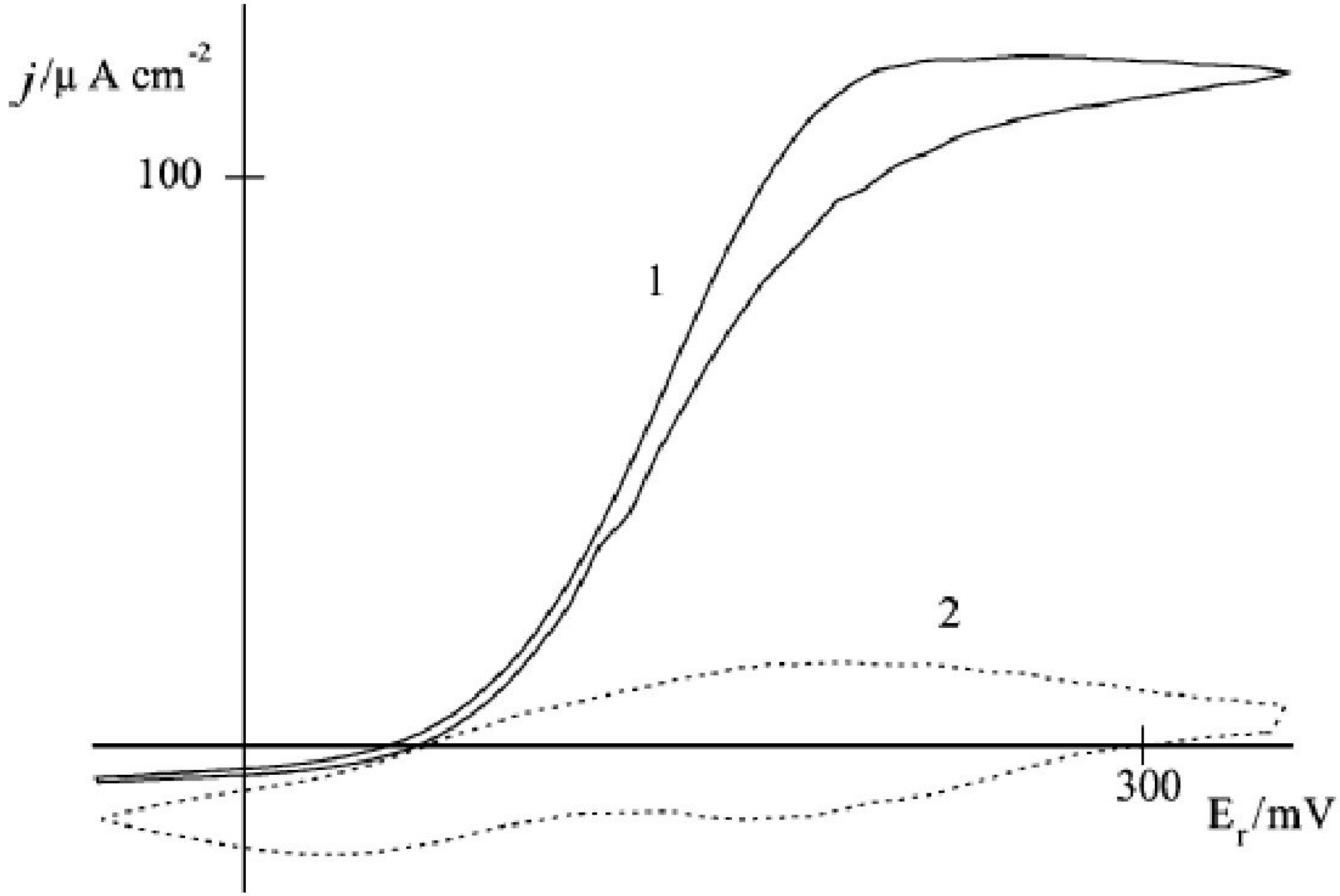

Fig. 2. Hydrogenase poly(CI) electrode (type II) in H_2 (1) and Ar (2).

Циклическая вольтамперометрия
(адсорбция)

$$i_p = \frac{n^2 F^2}{4RT} A \Gamma v$$

$$E_p = E^{0\prime} - \frac{RT}{nF} \ln \frac{b_O}{b_R}$$

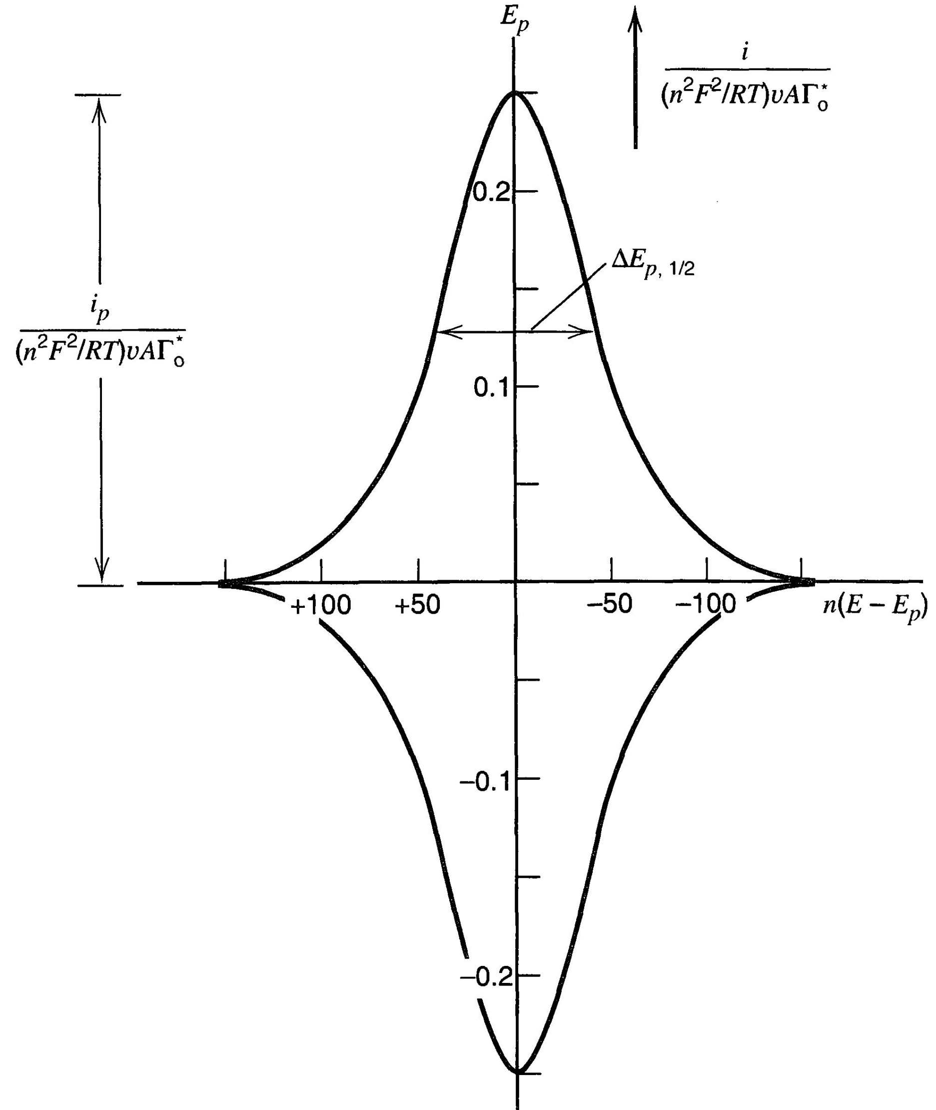

Циклическая вольтамперометрия
(влияние адсорбции)

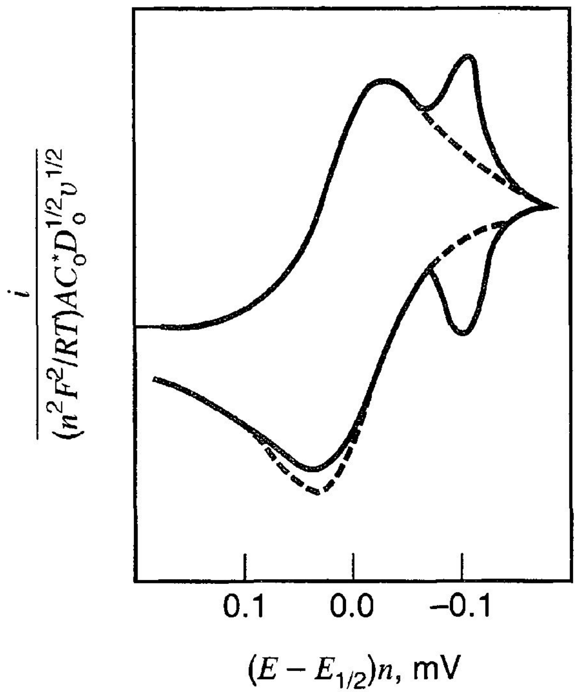

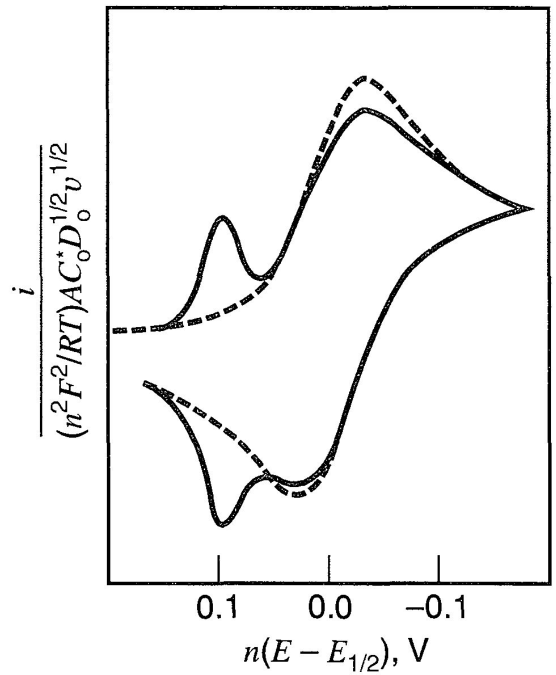

Циклическая вольтамперометрия (влияние адсорбции)

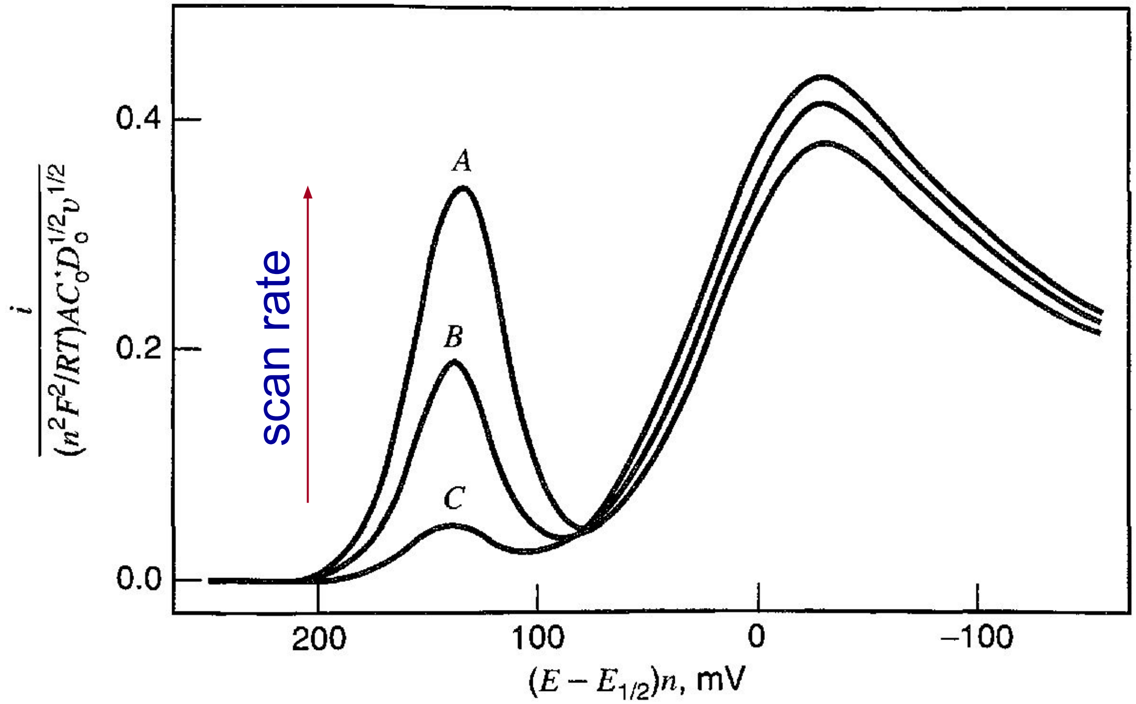

Циклическая вольтамперометрия
(влияние адсорбции)

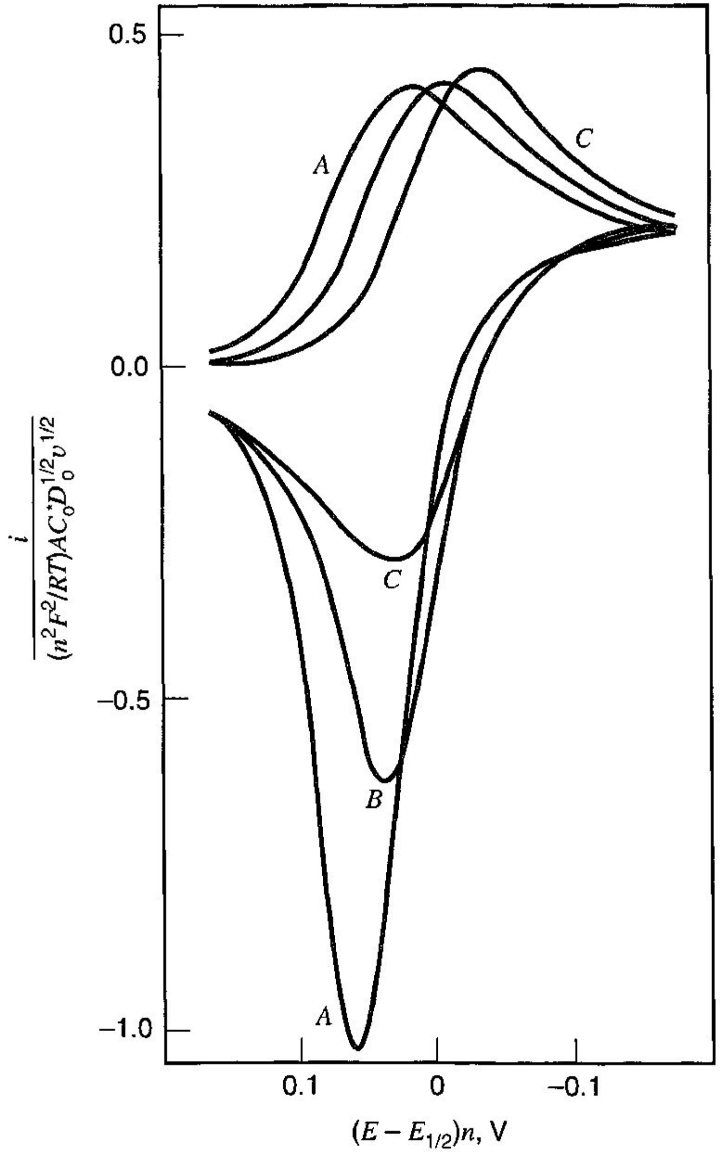

Посадка-снятие оксидного слоя Au

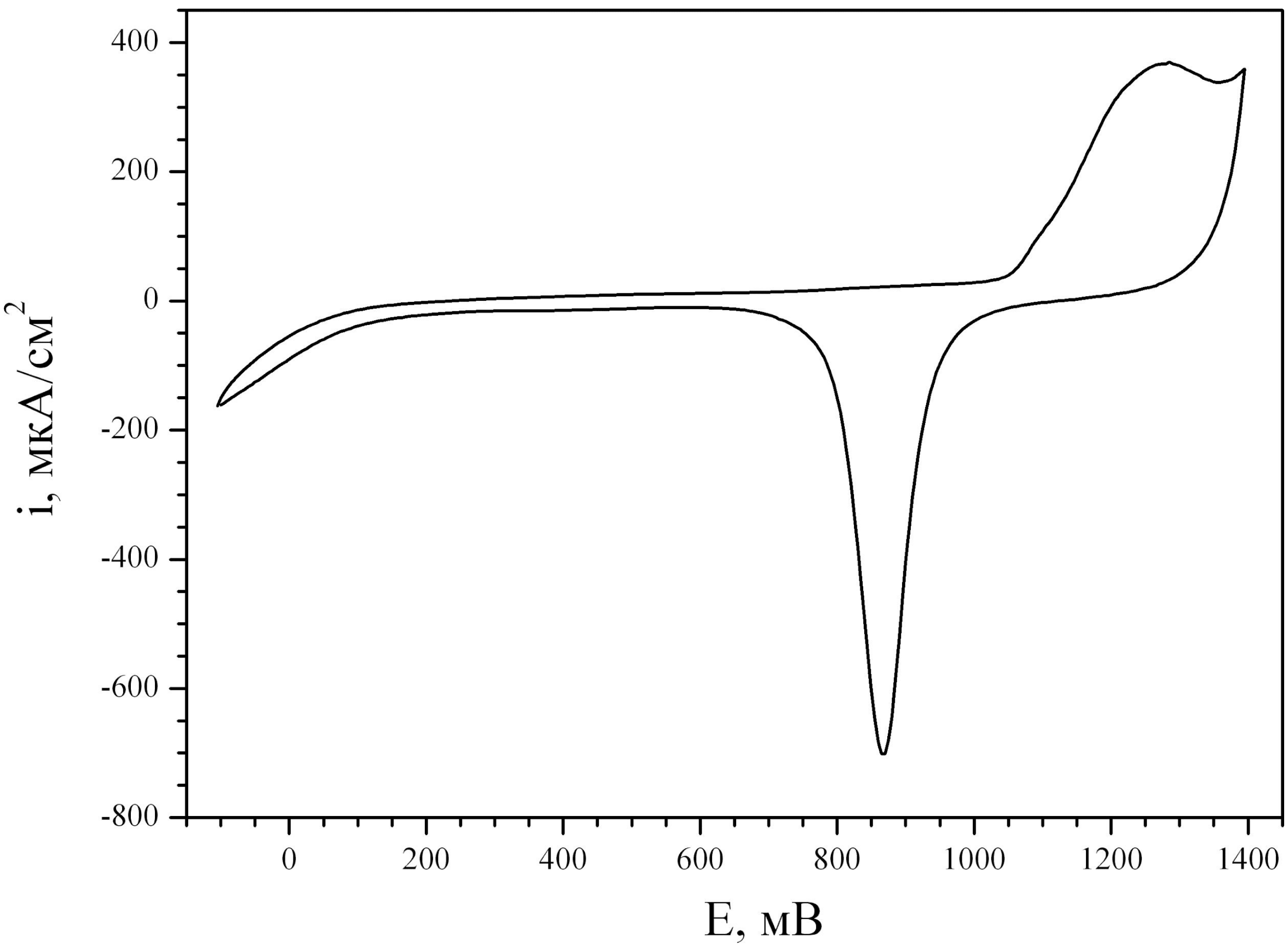

Берлинская лазурь

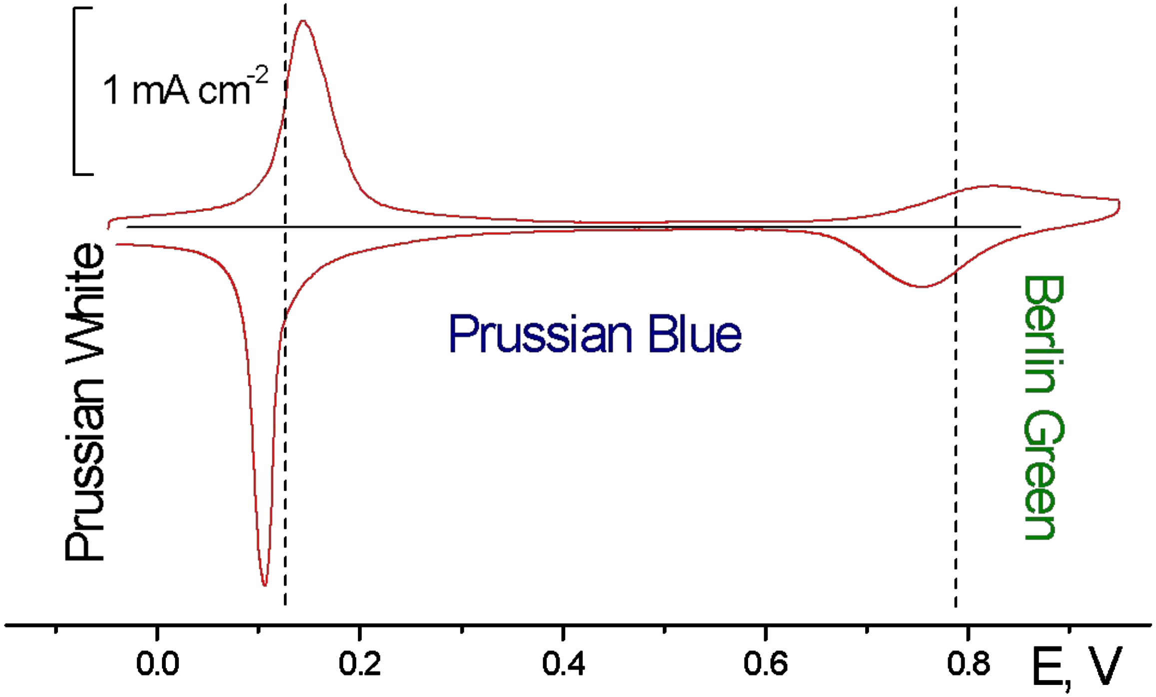

Электрополимеризация

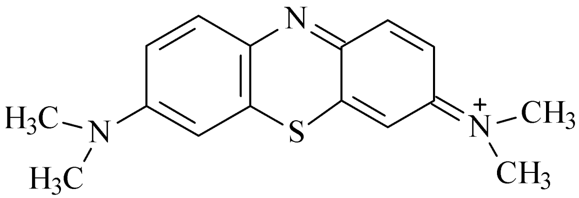

Methylene Blue

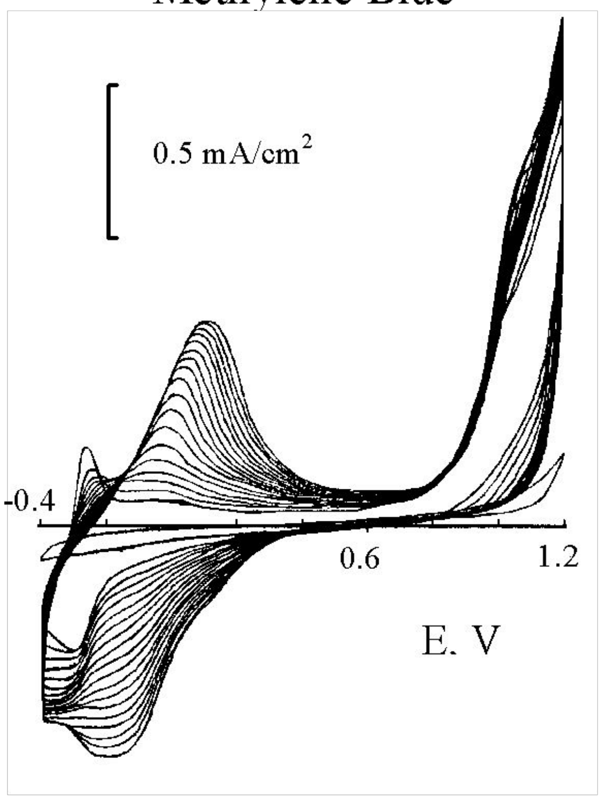

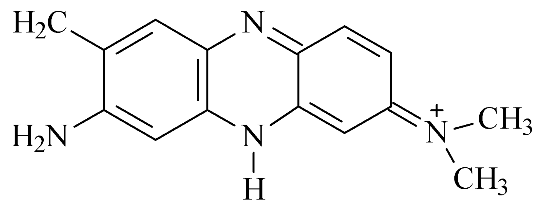

Neutral Red

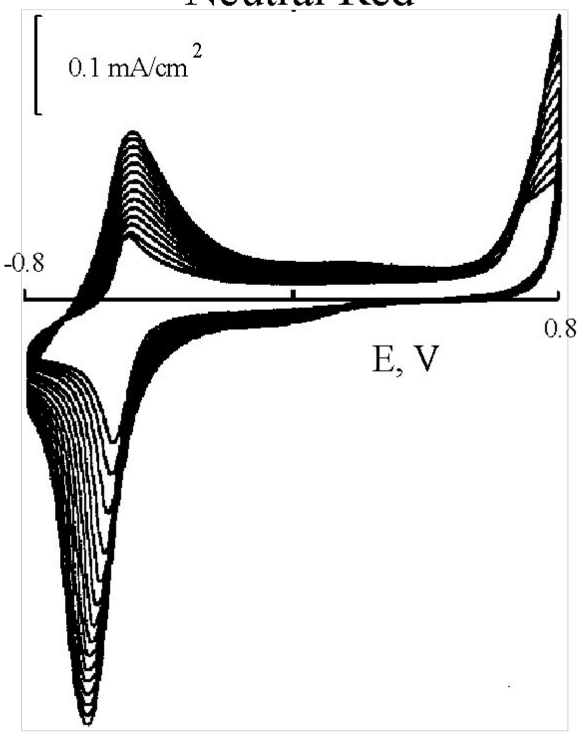

ОБРАТИМЫЙ ПЕРЕНОС ЭЛЕКТРОНА С ЦИТОХРОМА С НА ПОВЕРХНОСТЬ ЭЛЕКТРОДА

REVERSIBLE ELECTRODE REACTION OF CYTOCHROME c

Peter YEH and Theodore KUWANA
Department of Chemistry
The Ohio State University
Columbus, OHIO 43210 USA

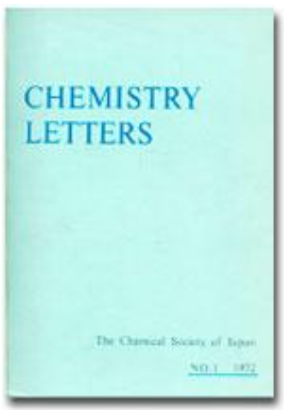

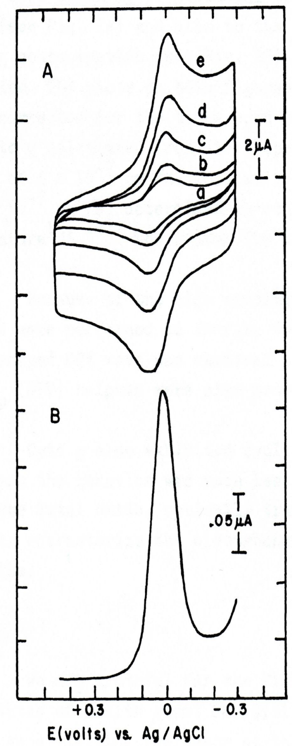

Fig. 1 A. Cyclic i-E curves of 52 μM cyto c at 10, 20, 50, 100, and 200 (a to e) mV/s. B. Differential pulse i-E curve of 20 μM cyto c at 2 mV/s scan rate, 50 mV pulse height, and 0.5 s pulse width.

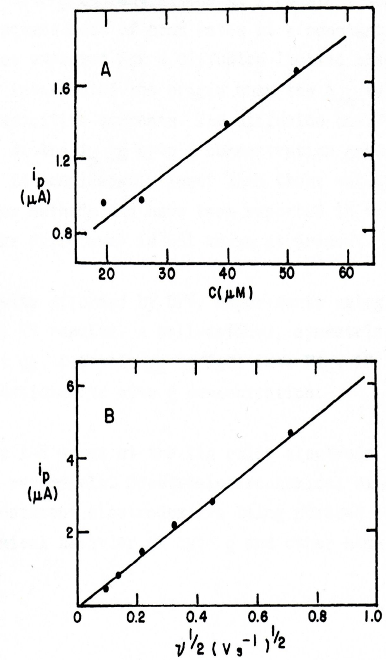

Fig. 2 A. Plot of cyclic peak currents (at 50 mV/s) as a function of cyto c concentration. B. Plot of cyclic peak currents as a function of scan rate (52 μM cyto c).

The heme protein, cytochrome c, was found to exhibit reversible electron transfer characteristics at an indium oxide electrode. The electrode reaction at this electrode was evaluated using cyclic voltammetry and differential pulse method.

CHEMISTRY LETTERS, pp. 1145-1148, 1977. Published by the Chemical Society of Japan

ОБРАТИМЫЙ ПЕРЕНОС ЭЛЕКТРОНА С ЦИТОХРОМА С НА ПОВЕРХНОСТЬ ЭЛЕКТРОДА

Novel Method for the Investigation of the Electrochemistry of Metalloproteins: Cytochrome c

By Mark J. Eddowes and H. Allen O. Hill*
(*Inorganic Chemistry Laboratory, South Parks Road, Oxford* OX1 3QR)

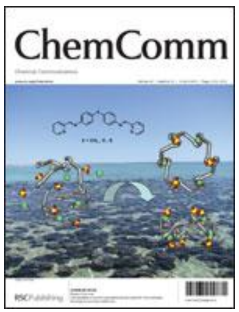

J. Chem. Soc. , Chem. Commun. (**1977**) 71

Summary The d.c. and a.c. cyclic voltammetries of horse heart ferricytochrome c have been investigated and it is shown that, in the presence of 4,4′-bipyridyl, the electrochemistry corresponds to a quasi-reversible one-electron process, from which an $E°$ value of $+0·25$ V *vs.* normal hydrogen electrode can be derived.

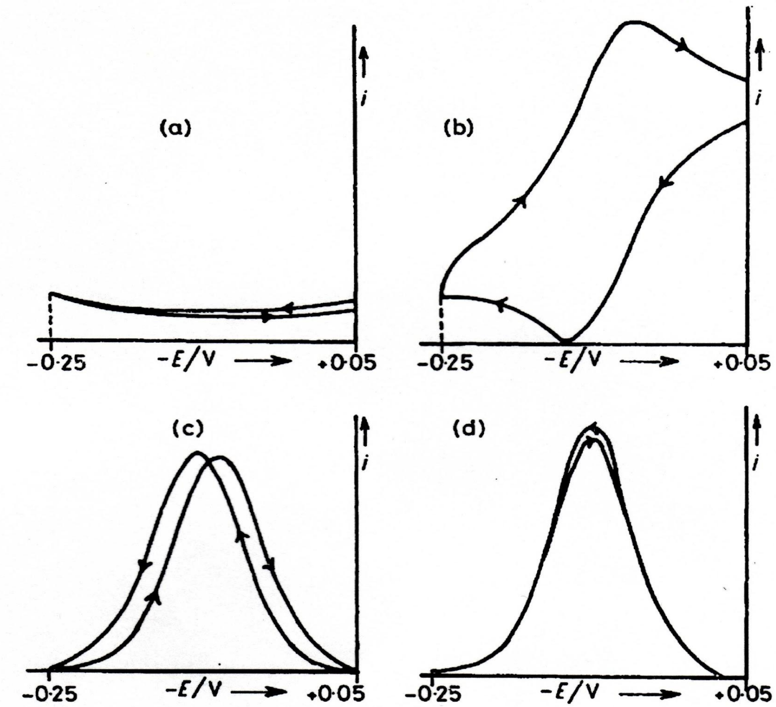

FIGURE. Cyclic voltammograms of an aqueous solution of horse heart ferricytochrome c (2 mM), containing $NaClO_4$ (0·1 M), and Na_2HPO_4 (0·02 M), pH 7, at a planar gold disc electrode in the potential range + 0·05 to −0·25 V *vs.* 0·1 M KCl–calomel ($E°$ + 0·336 V *vs.* NHE). (a) A.c. cyclic voltammogram at a scan rate of 10 mV s^{-1} in the absence of 4,4′-bipyridyl; (b) d.c. cyclic voltammogram at a scan rate of 10 mV s^{-1} in the presence of 4,4′-bipyridyl (5 mM); (c) a.c. cyclic voltammogram at a scan rate of 10 mV s^{-1} in the presence of 4,4′-bipyridyl (5 mM); (d) a.c. cyclic voltammogram at a scan rate of 2·5 mV s^{-1} in the presence of 4,4′-bipyridyl (5 mM).

J.C.S. Chem. Comm., 1977

Наночастицы

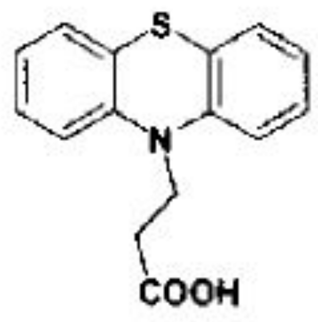

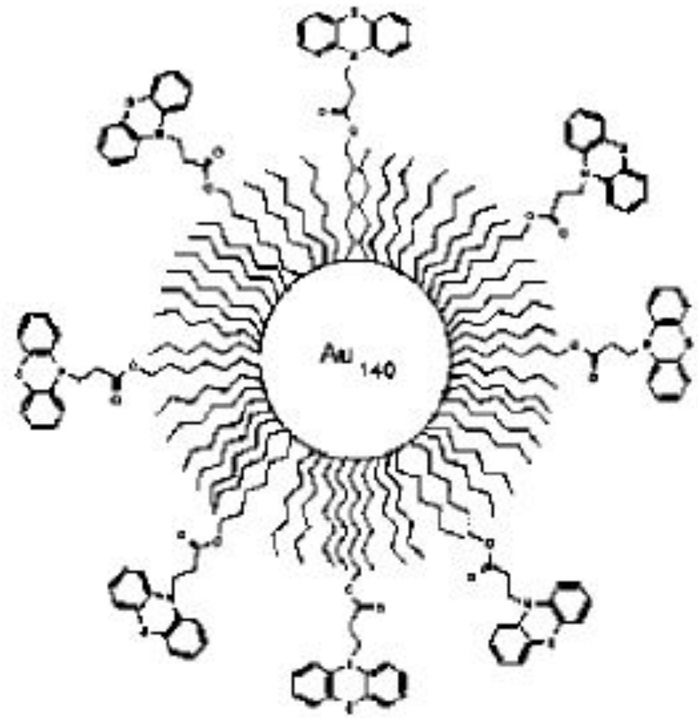

Royce W. Murray *Chem. Rev.* **2008,** *108,* 2688–2720

Наночастицы

Au_{140} MPC

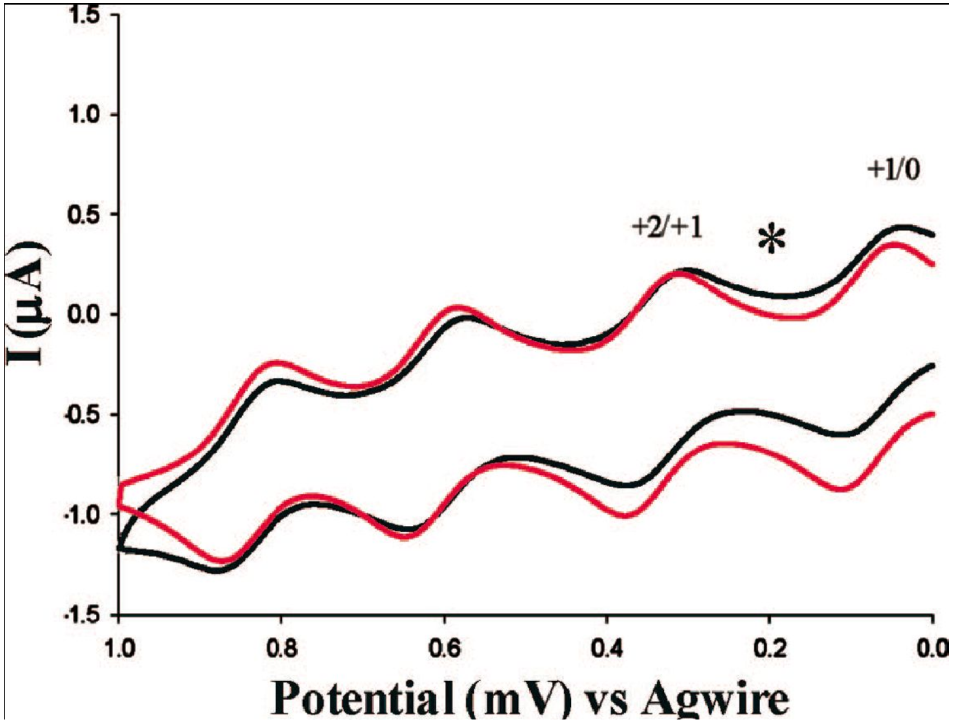

Royce W. Murray *Chem. Rev.* **2008,** *108,* 2688–2720

Наночастицы

Au_{25} MPC

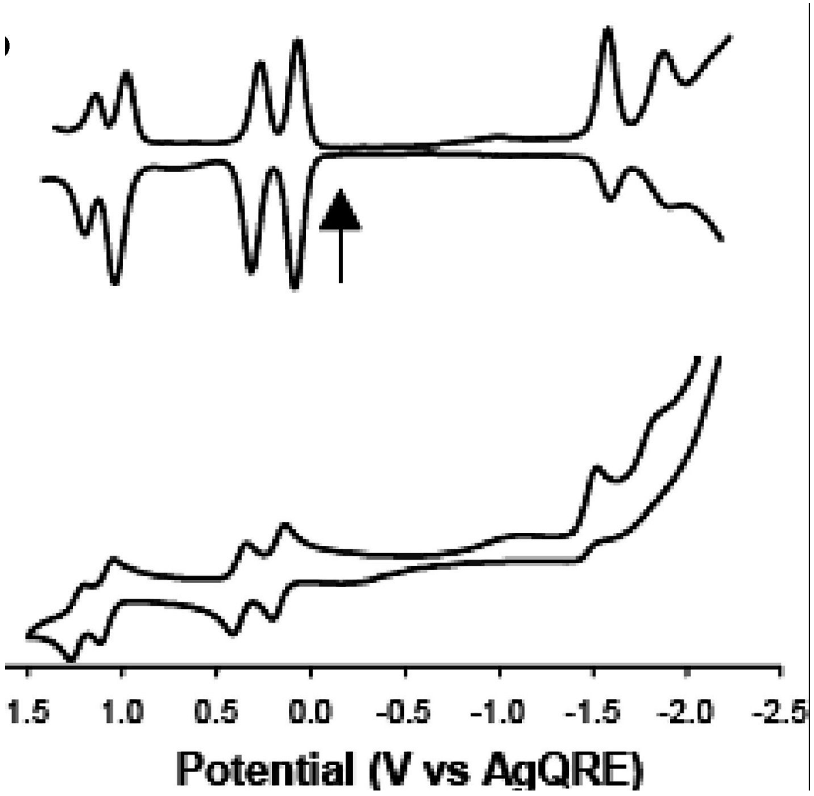

Royce W. Murray *Chem. Rev.* **2008,** *108,* 2688–2720

Наночастицы

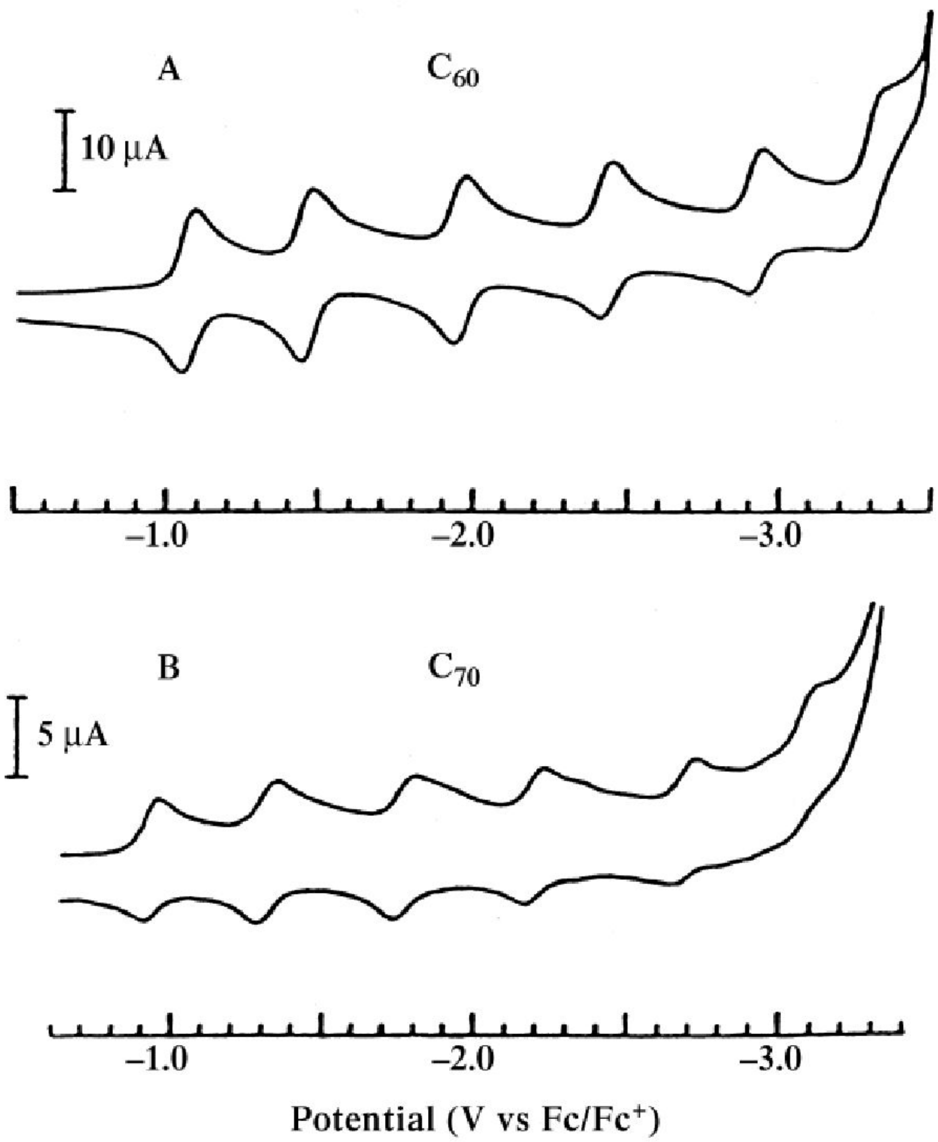

Инверсионная вольтамперометрия (stripping voltammetry)

Анодная инверсионная вольтамперометрия

1. Преконцентрирование:

$$Me^{n+} + n\bar{e} + Hg \rightarrow Me(Hg)$$

от 30 сек. для 10^{-7} М до 20 мин. для 10^{-10} М

2. Определение:

- линейная развертка потенциала,
- дифференциальная импульсная или квадратноволновая вольтамперометрия

Анодная инверсионная вольтамперометрия

Анодная инверсионная вольтамперометрия

$$C_{Hg} = \frac{i_l t_d}{nFV_{Hg}}$$

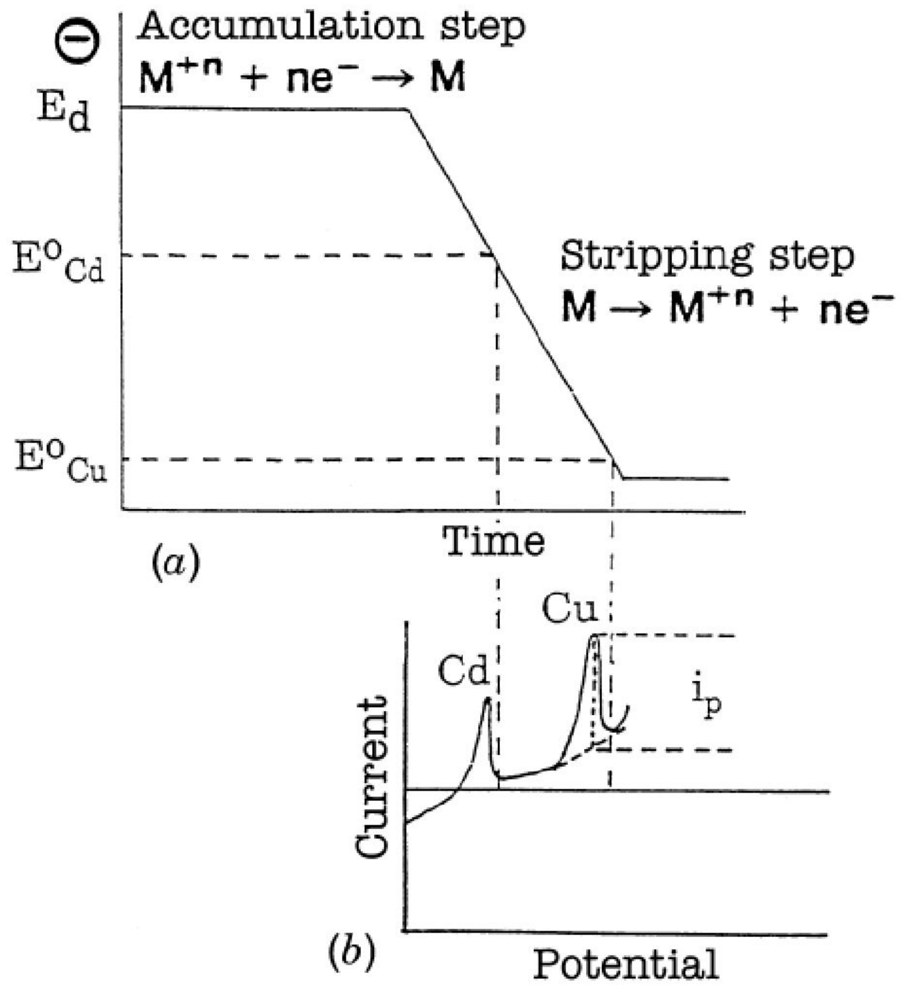

Анодная инверсионная вольтамперометрия

$$i_p = \frac{n^2 F^2 A l C_{Hg}}{2.7RT} v^{\varphi}$$

$i_p \propto v^{1/2}$ — большие v и l

$i_p \propto v$ — малые v и l

Анодная инверсионная вольтамперометрия

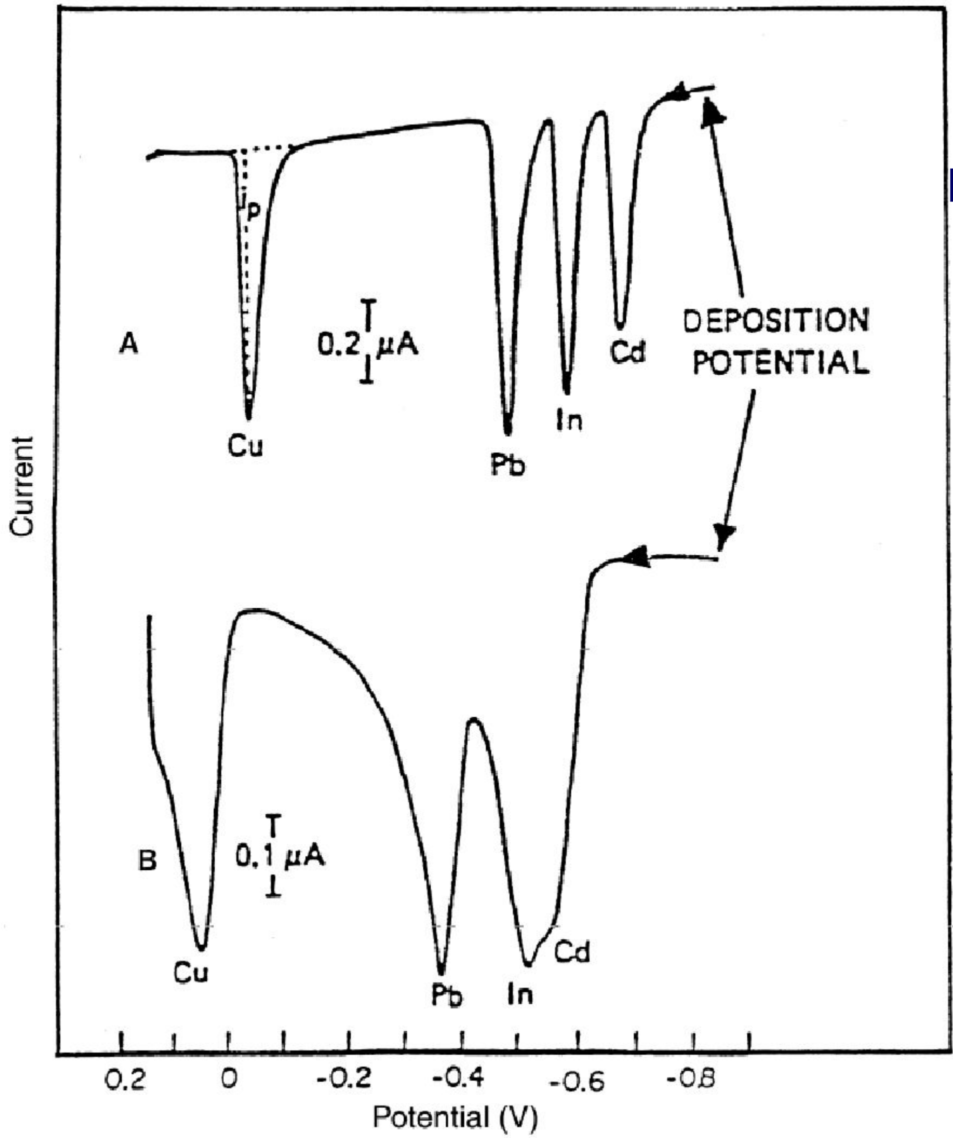

пленка

капля

Адсорбционная инверсионная вольтамперометрия

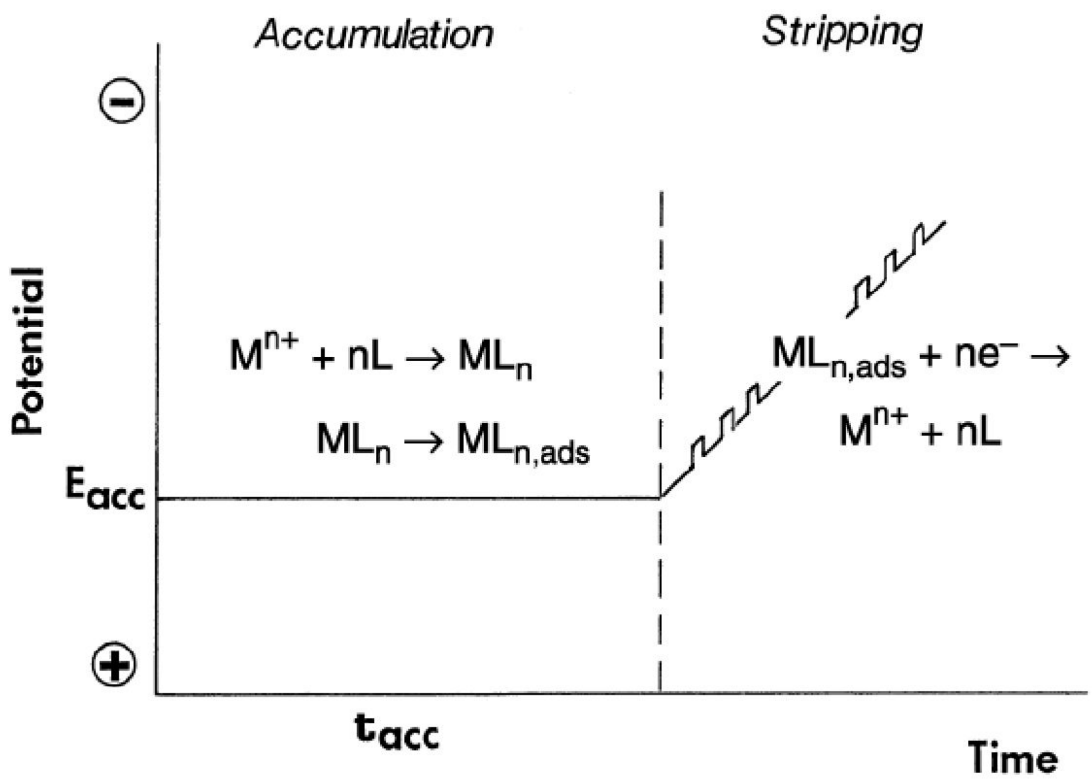

Адсорбционная инверсионная вольтамперометрия

Metal	Complexing Agent	Supporting Electrolyte	Detection Limit, (M)
Al	Dihydroxyanthraquinone-sulfonic acid	BES buffer	1×10^{-9}
Be	Thorin	Ammonia buffer	3×10^{-9}
Co	Nioxime	Hepes buffer	6×10^{-12}
Cr	Diethylenetriamine-Pentaacetic acid	Acetate buffer	4×10^{-10}
Fe	Solochrome violet RS	Acetate buffer	7×10^{-10}
Mn	Eriochrome Black T	Pipes buffer	6×10^{-10}
Mo	Oxine	Hydrochloric acid	1×10^{-10}
Ni	Dimethylglyoxime	Ammonia buffer	1×10^{-10}
Pt	Formazone	Sulfuric acid	1×10^{-12}
Sn	Tropolone	Acetate buffer	2×10^{-10}
Ti	Mandelic acid	Potassium chlorate	7×10^{-12}
U	Oxine	Pipes buffer	2×10^{-10}
V	Catechol	Pipes buffer	1×10^{-10}

Катодная инверсионная вольтамперометрия

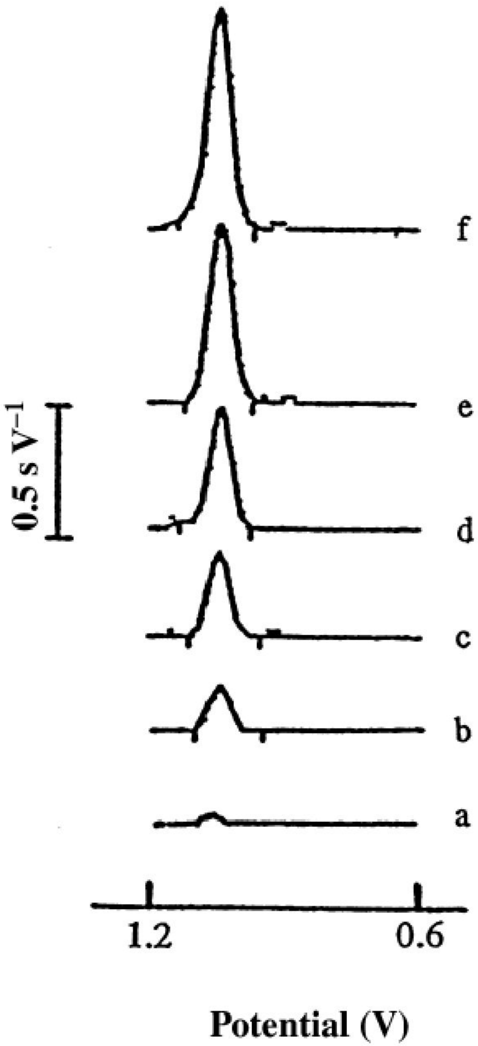

DNA 0.5 ppm

1÷150 с времена накопления

Abbe Limit

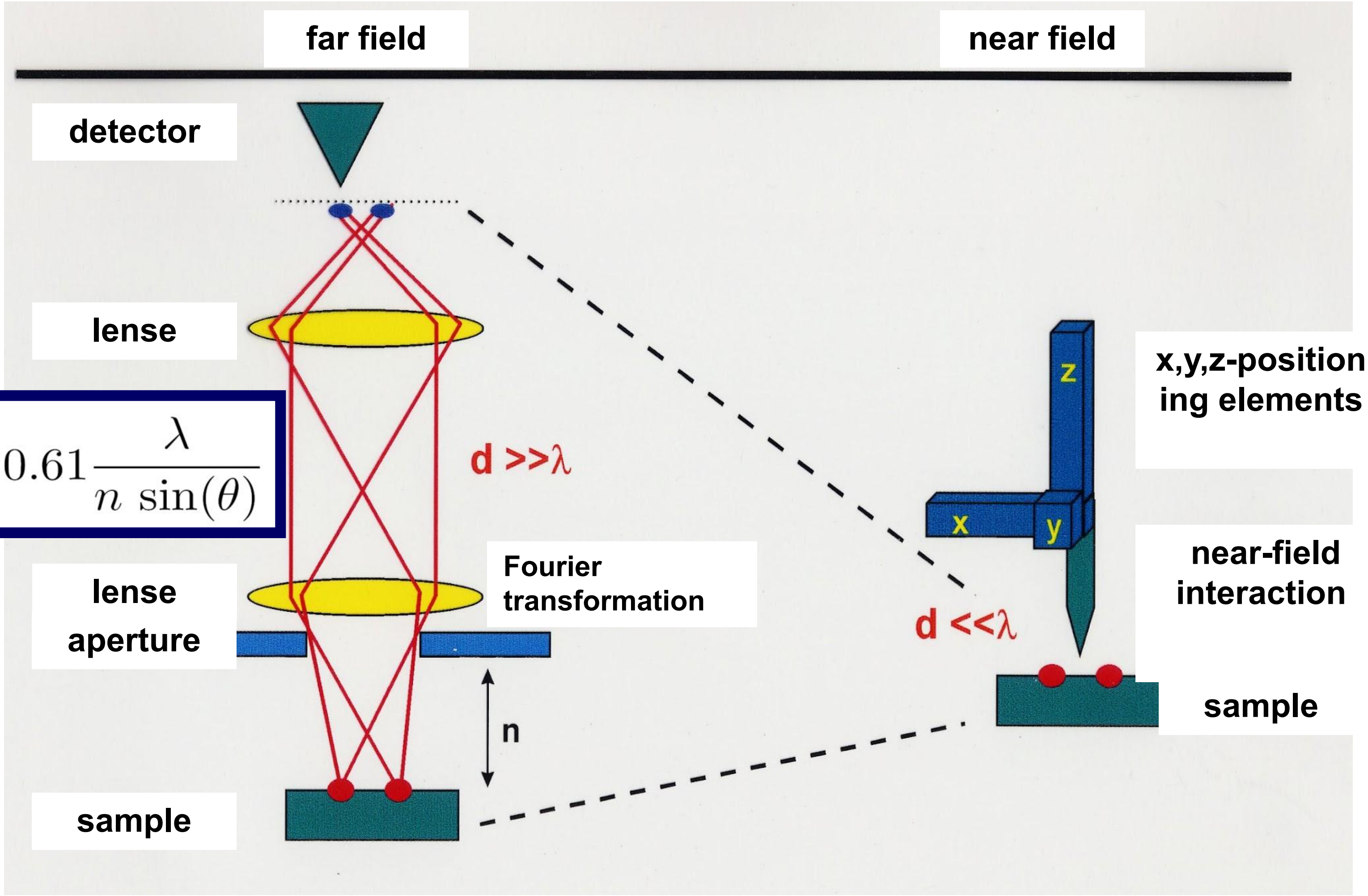

$$\Delta x \sim 0.61 \frac{\lambda}{n \sin(\theta)}$$

Scanning Probe Microscopy - History

1981: scanning tunneling microscopy (STM)
(Binnig et al., *Helv. Phys. Acta,* 55 (1982) 726)

1984: near-field scanning microscopy (SNOM, NSOM)
(Pohl et al., *Appl. Phys. Lett.,* 44 (1984) 651)

1986: atomic force microscopy (AFM)
(Binnig, G.; Quate, C. F.; Gerber, C., *Phys. Rev. Lett.* 56 (1986) 930)

1986: nobel prize for G. Binnig, H. Rohrer, H. Ruska

1988: first commercial AFM

1989: scanning electrochemical microscopy (SECM)
(A. J. Bard, F. F. Fan, J. Kwak, O. Lev, *Anal. Chem.* 61 (1989) 132; R. C. Engstrom, C. M. Pharr, *Anal. Chem.* 61 (1989) A1099)

History - Probing diffusion layers

Spatiotemporal Description of the Diffusion Layer with a Microelectrode Probe

Royce C. Engstrom,* Trevor Meaney, and Ray Tople
Department of Chemistry, University of South Dakota, Vermillion, South Dakota 57069

R. Mark Wightman
Department of Chemistry, Indiana University, Bloomington, Indiana 47405

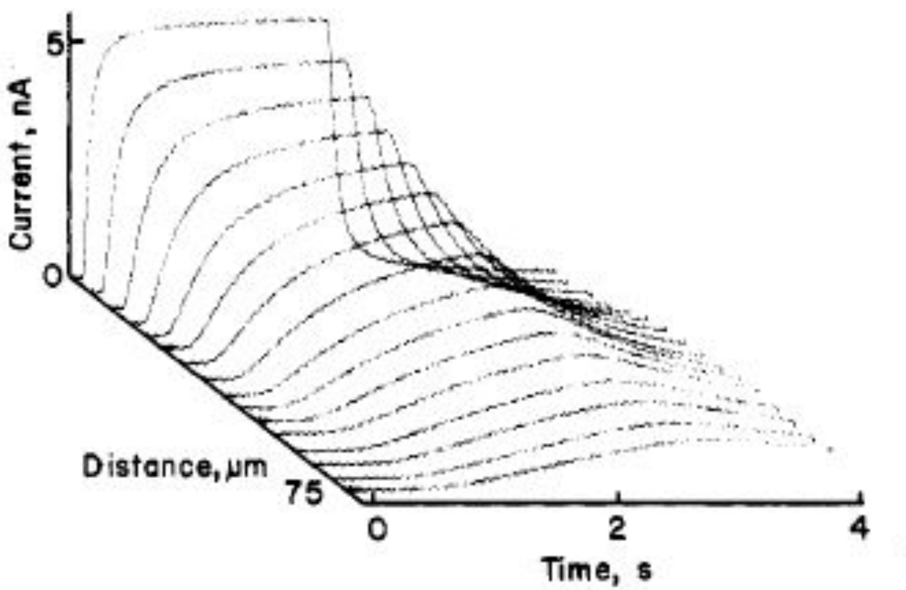

Figure 2. Current–time response of microelectrode at various inter-electrode distances.

Royce C. Engstrom, Trevor Meaney, Ray Tople, R. Mark Wightman *Anal. Chem.* **59** (1987), 2005
Spatiotemporal Description of the Diffusion Layer with a Microelectrode Probe

History - Introduction & principles of SECM - I

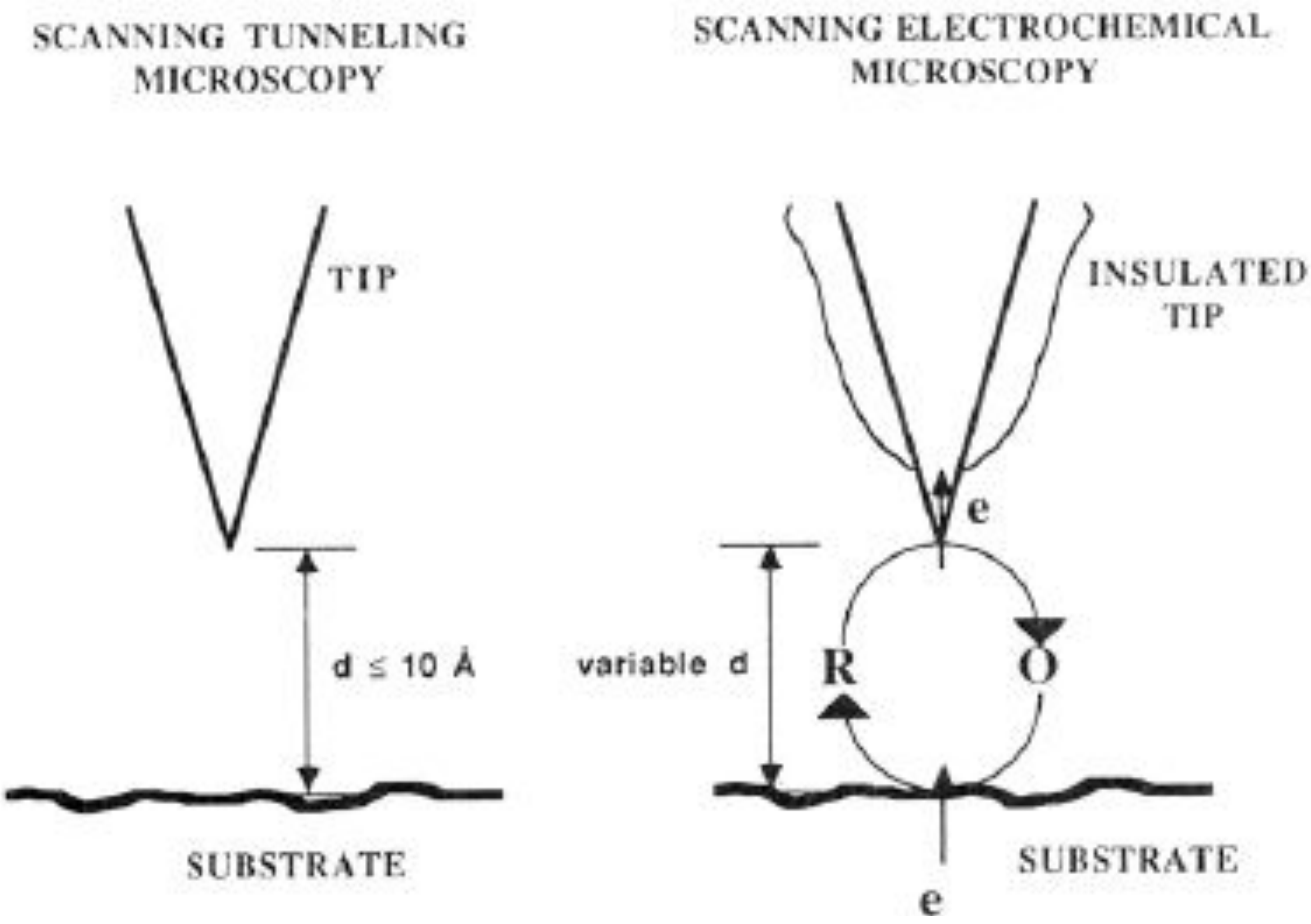

A.J. Bard, F.R.F. Fan, J. Kwak, O. Lev *Anal. Chem.* **61** (1989), 132 *Scanning Electrochemical Microscopy. Introduction and Principles*

Positive Feedback Mode (Redox Recycling)

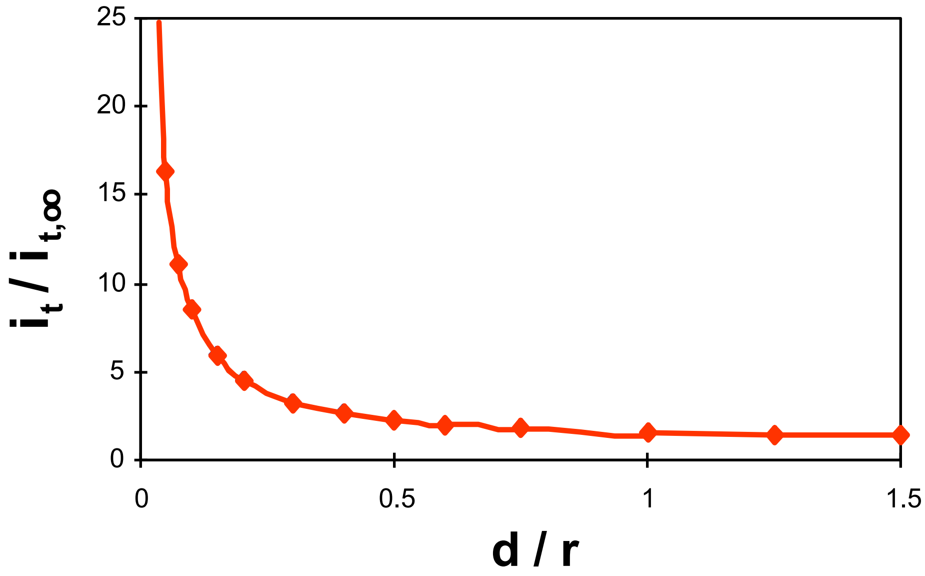

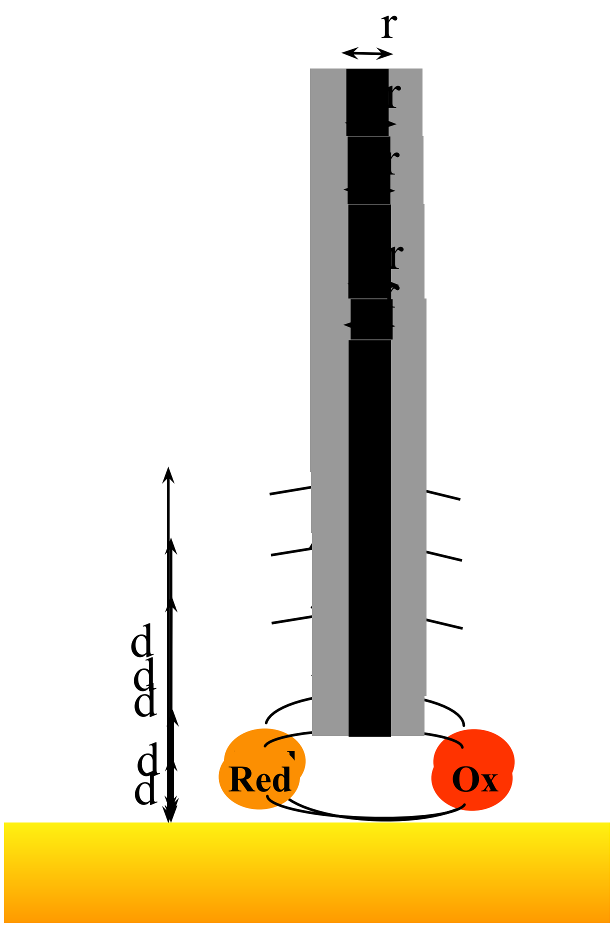

Negative Feedback Mode (Diffusion Blocking)

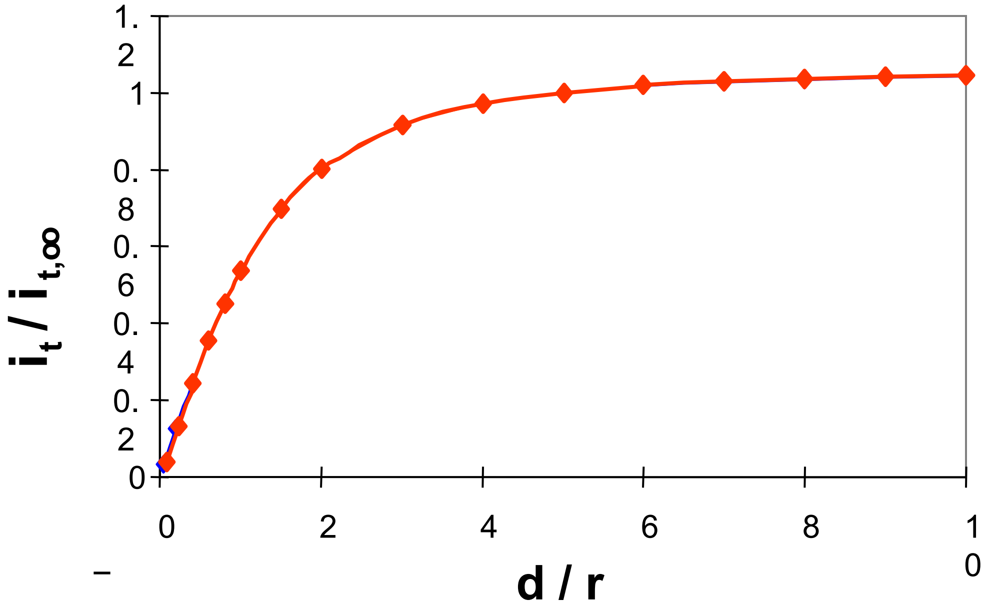

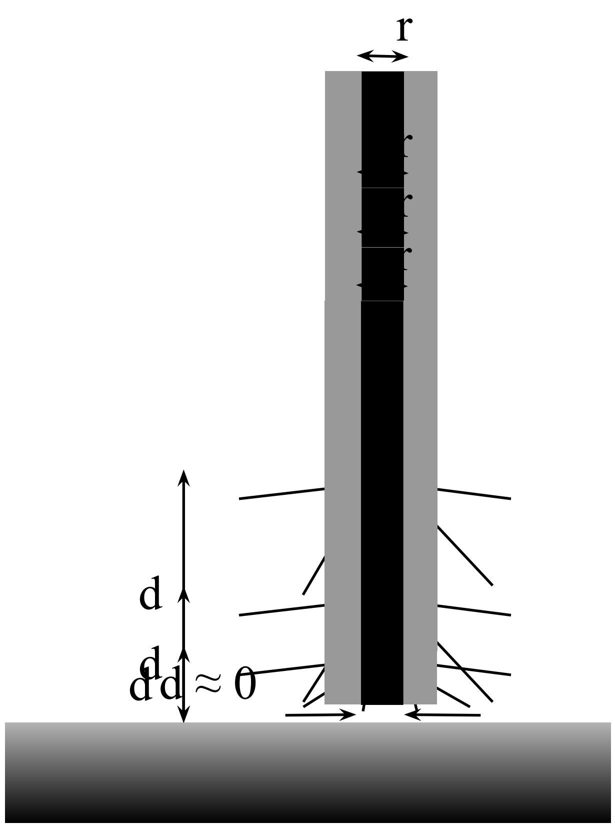

SECM - Working Modes

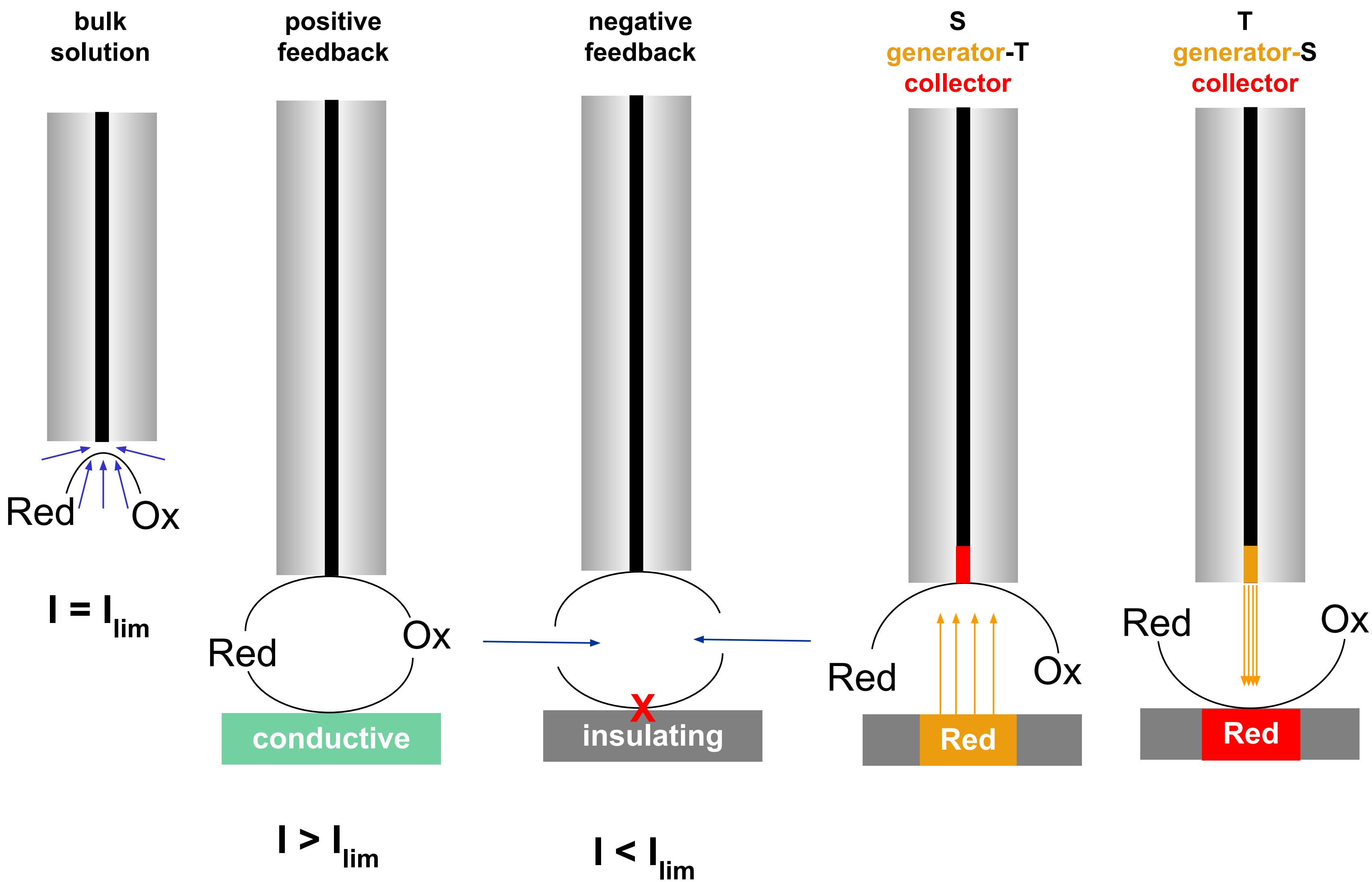

SECM tips

- **Metal Microelectrodes**
  - Disk-in-Glass Microelectrodes
  - Submicrometer Glass-Encapsulated Microelectrodes
  - Electrochemical Etching of Metal Wires
  - Self-Assembled Spherical Gold Microelectrodes
  - Mercury Mircoelectrodes

- **Carbon Microelectrodes**
  - Carbon Fiber Microelectrodes
    - Glass Encapsulation of Carbon Fiber Microelectrodes
    - Carbon Fiber Etching
  - Pyrolytic Carbon Microelectrodes

Pt-Nanoelectrodes

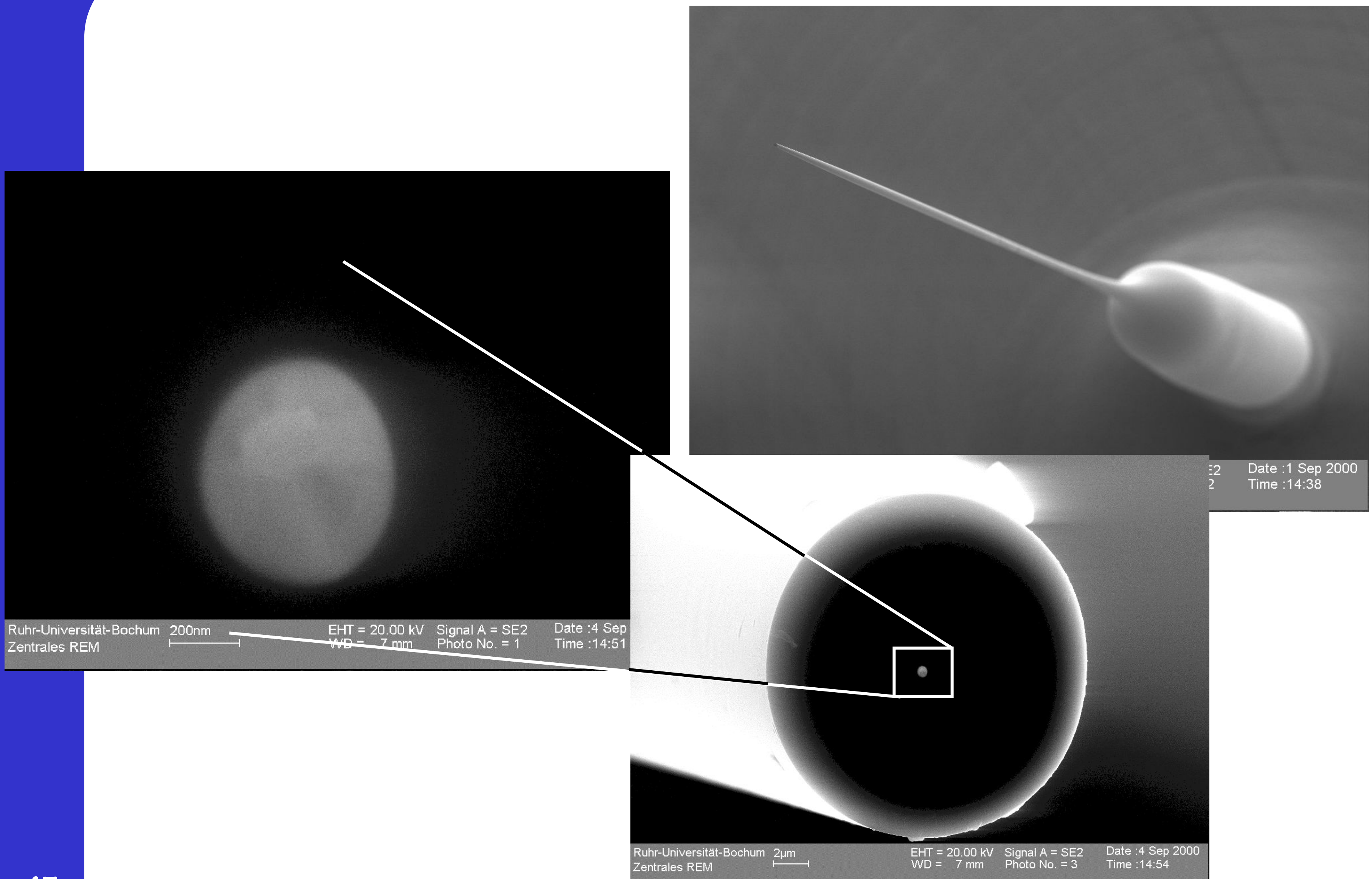

Characterization of Nanoelectrodes by Means of CV

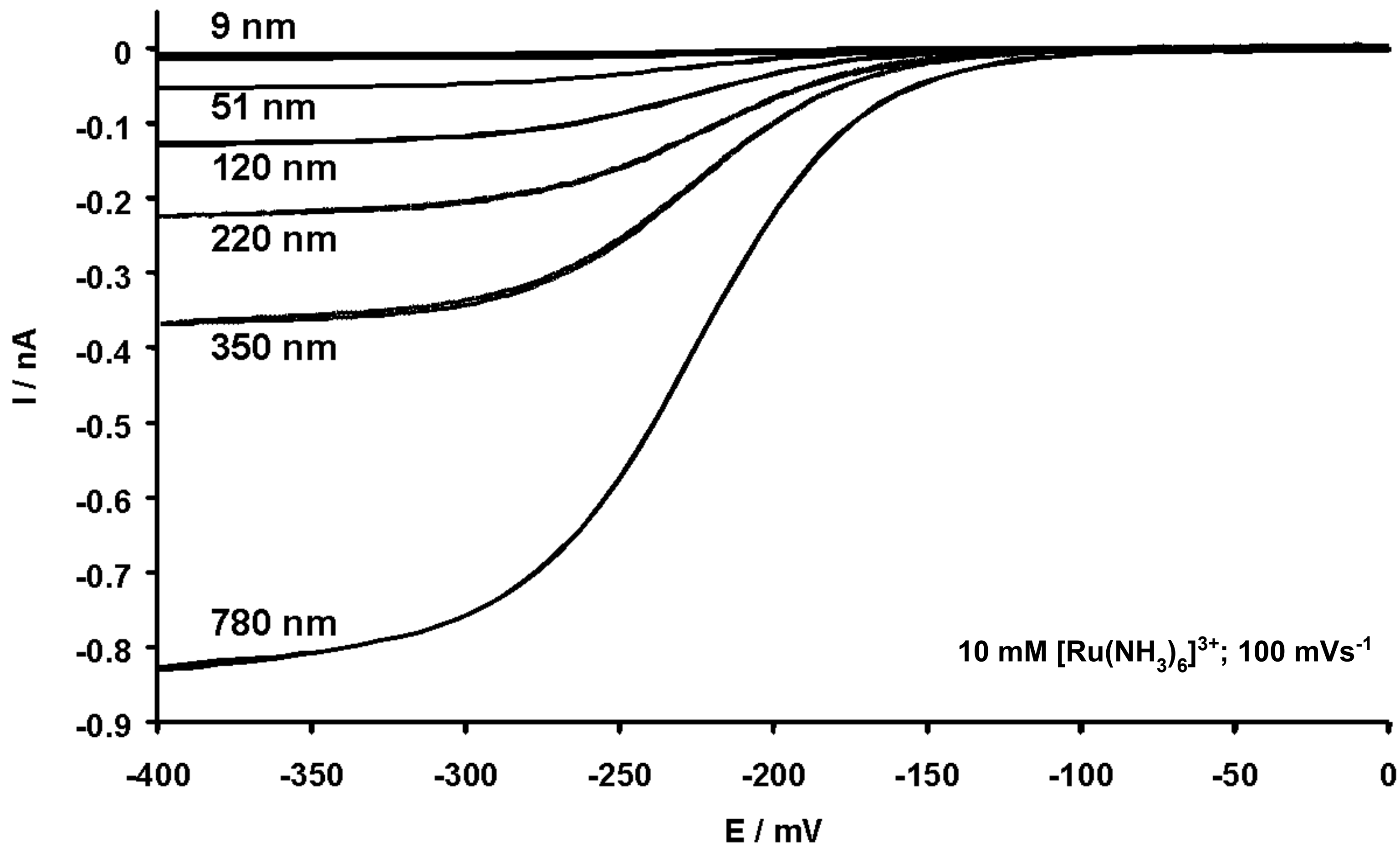

B. Ballesteros Katemann, W. Schuhmann, *Electroanalysis* **14** (2002) 22-28. Fabrication and Characterization of Needle-Type Pt-Disk Nanoelectrodes

SECM Approach Curves with Nanoelectrodes

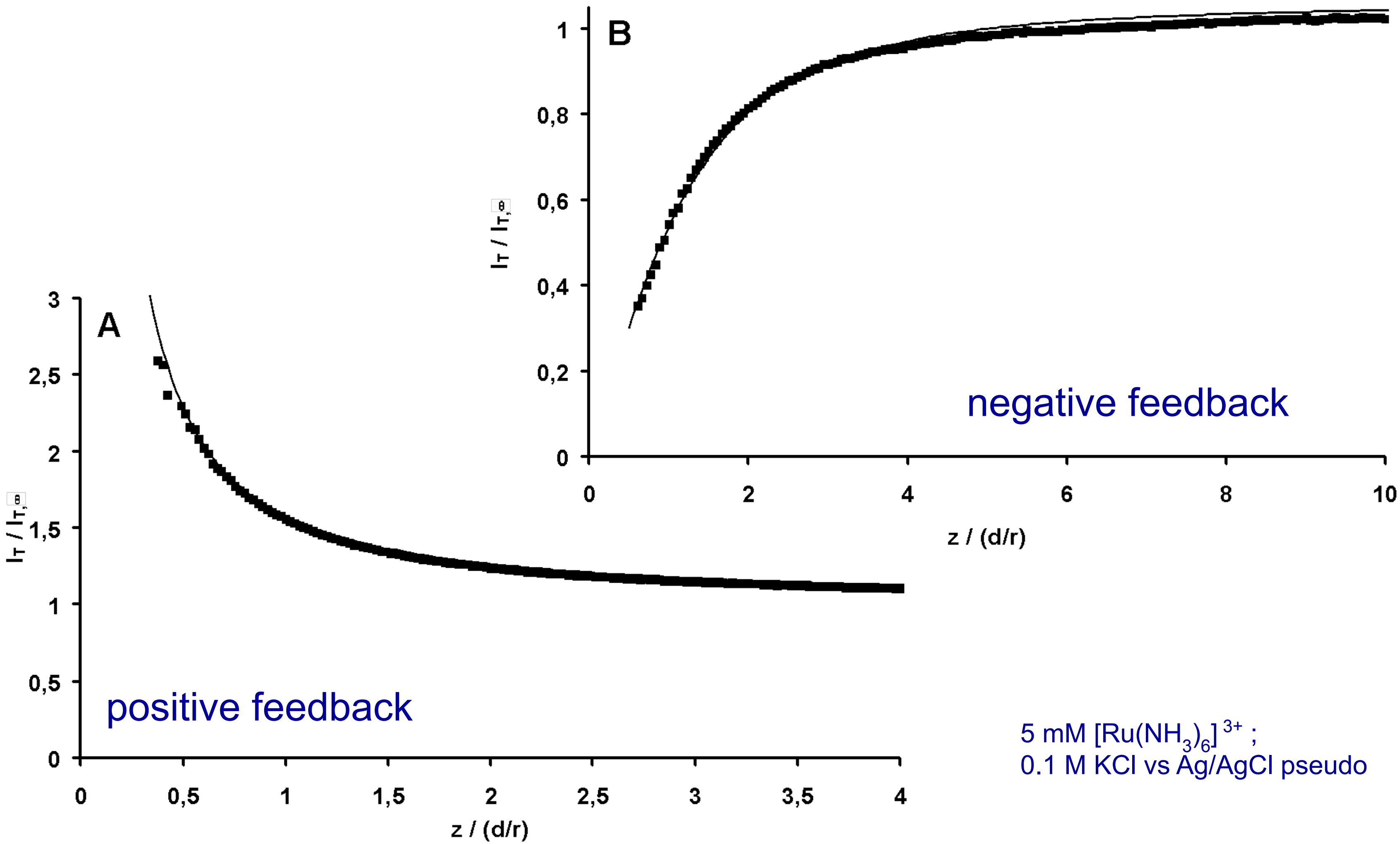

5 mM $[Ru(NH_3)_6]^{3+}$;
0.1 M KCl vs Ag/AgCl pseudo

B. Ballesteros Katemann, W. Schuhmann, *Electroanalysis* **14** (2002) 22-28. Fabrication and Characterization of Needle-Type Pt-Disk Nanoelectrodes

Scanning Electrochemical Microscopy - System Set-Up

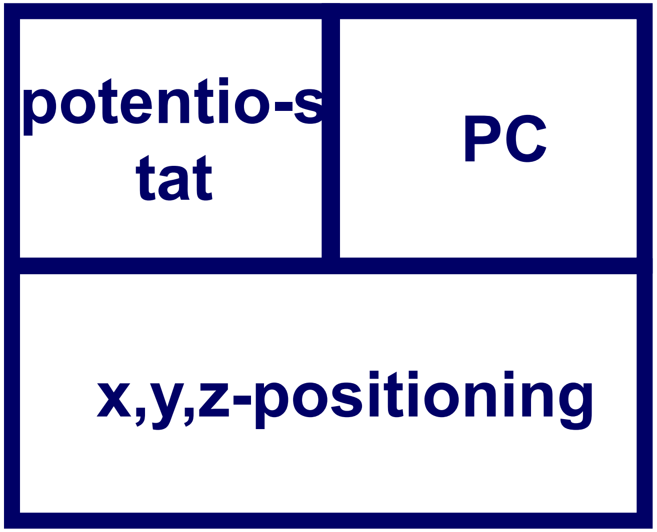

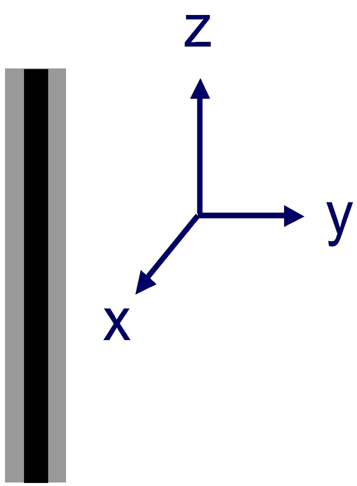

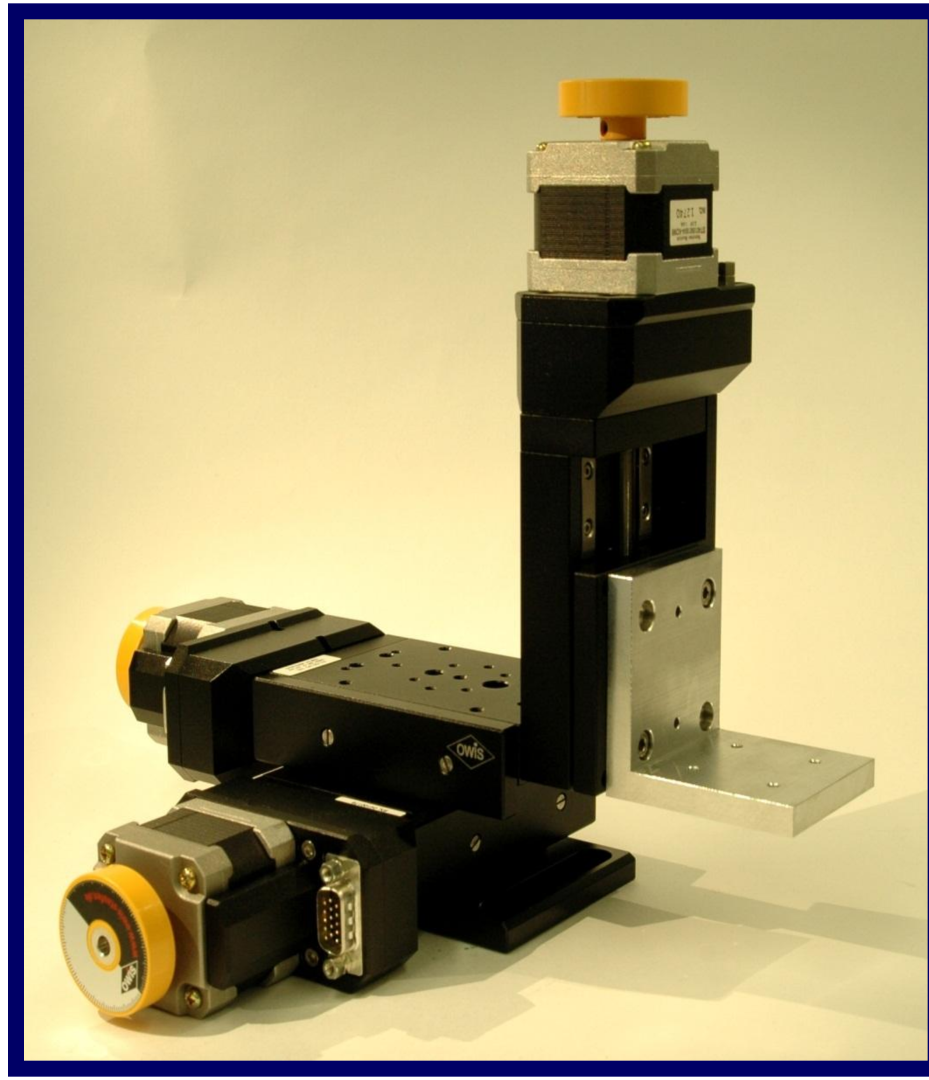

Scanning Electrochemical Microscopy - System Set-Up

Potentio-stat

PC

x,y,z-Positioning

Pt – band electrode. Constant Height Imaging

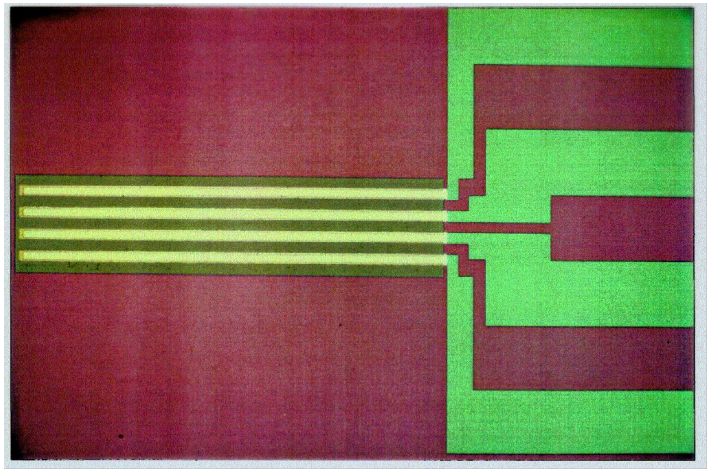

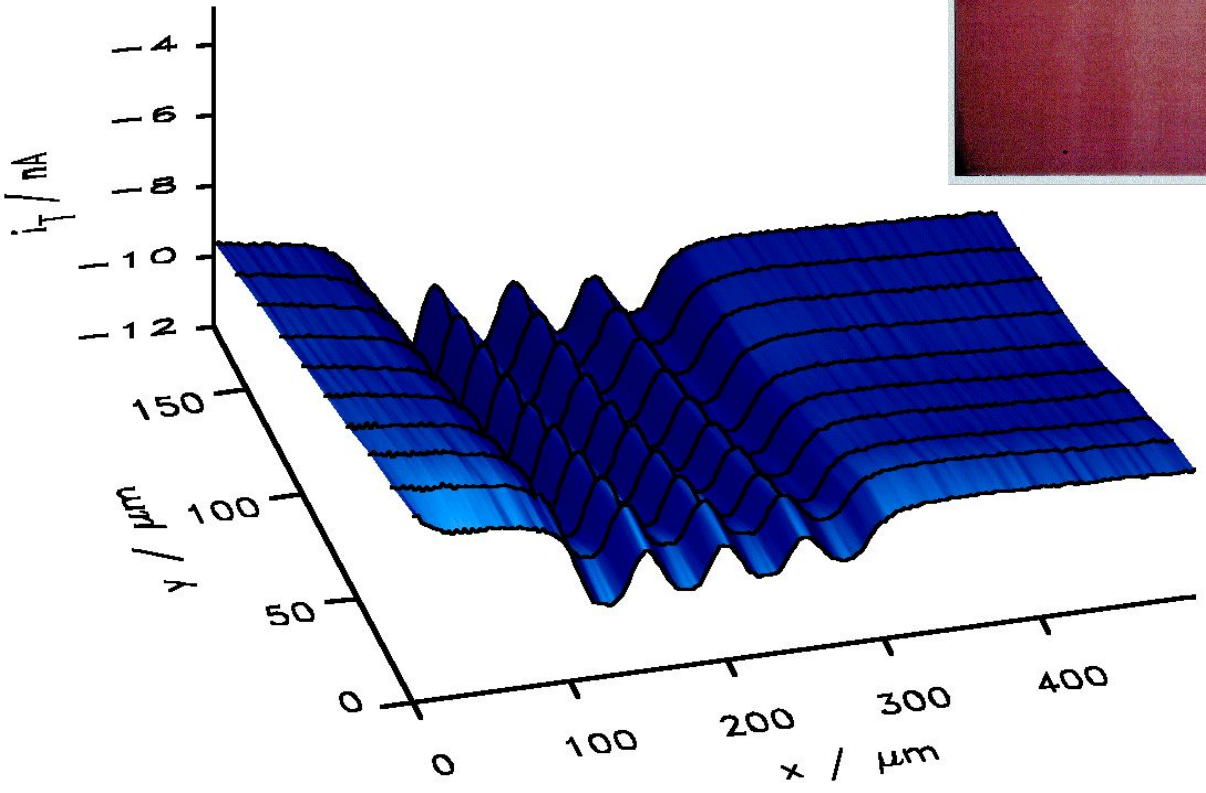

Sample supplied by Milena Koudelka-Hep, Institute of Microtechnology, Neuchatel, CH

Etching of Semiconductors - GaAs

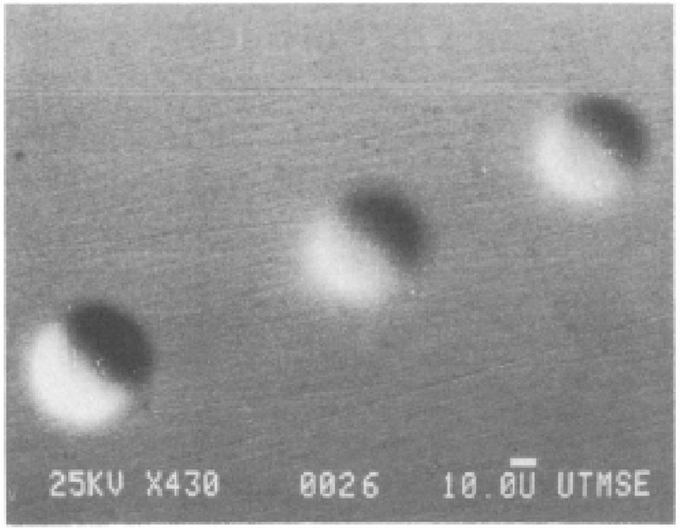

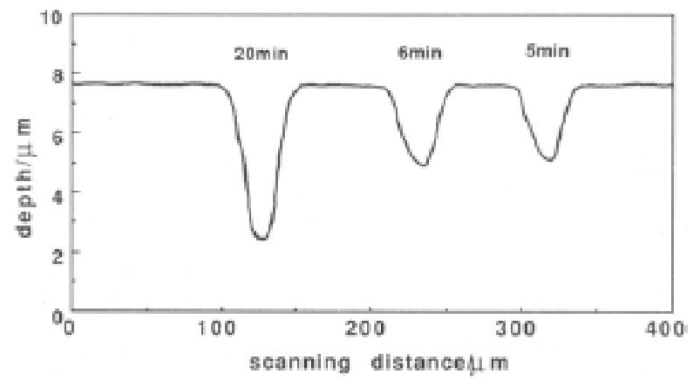

Fig. 2. (a, left) Scanning electron micrograph (SEM) of single crystal of GaAs etched in three places for 5, 6 and 20 min in a 0.02M HBr/0.1M HCl solution with a 25 μm Pt UME. (b, right) Profile of the GaAs surface at the etching spots.

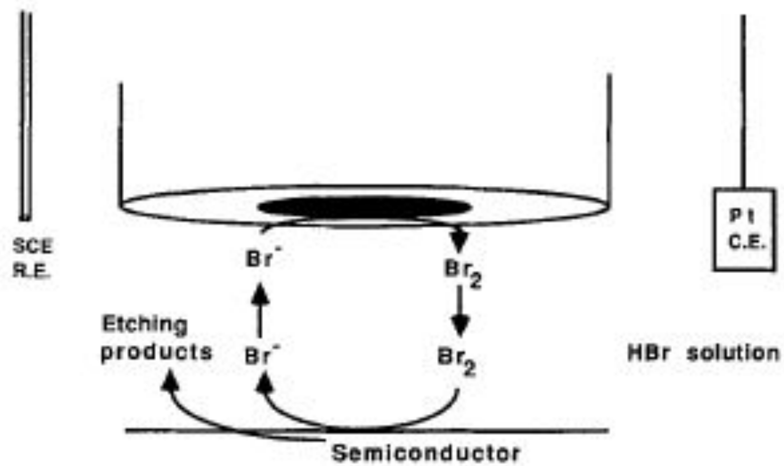

D. Mandler, A. J. Bard *J. Electrochem. Soc.* **137** (1990), 2468 *High Resolution Etching of Semiconductors by the Feedback Mode of the Scanning Electrochemical Microscope*

Deposition of Polypyrrol on Au

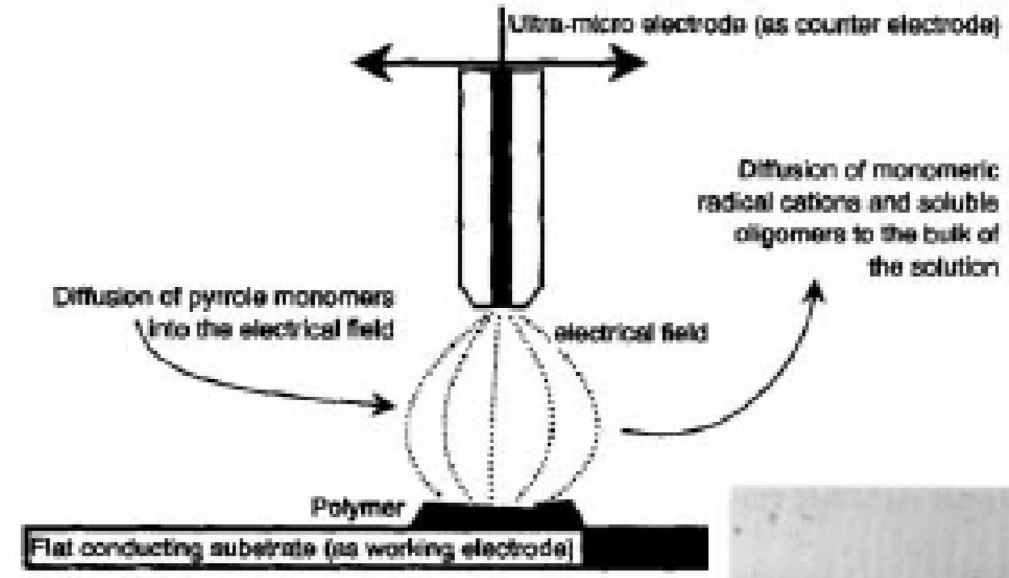

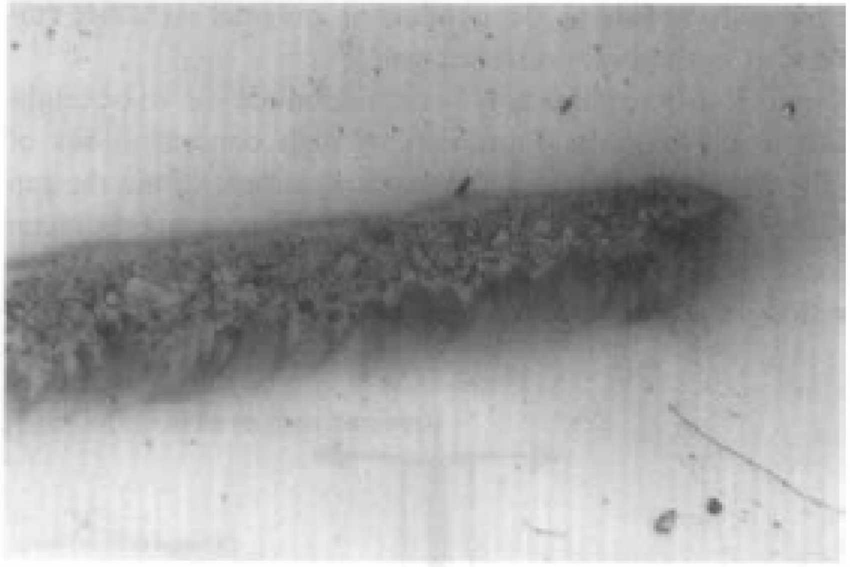

C. Kranz, M. Ludwig, H.E. Gaub, W. Schuhmann *Adv. Mater.* **7** (1995), 38 Lateral Deposition of Polypyrrole Lines by Means of the Scanning Electrochemical Microscope

Tip crash and surface tilt

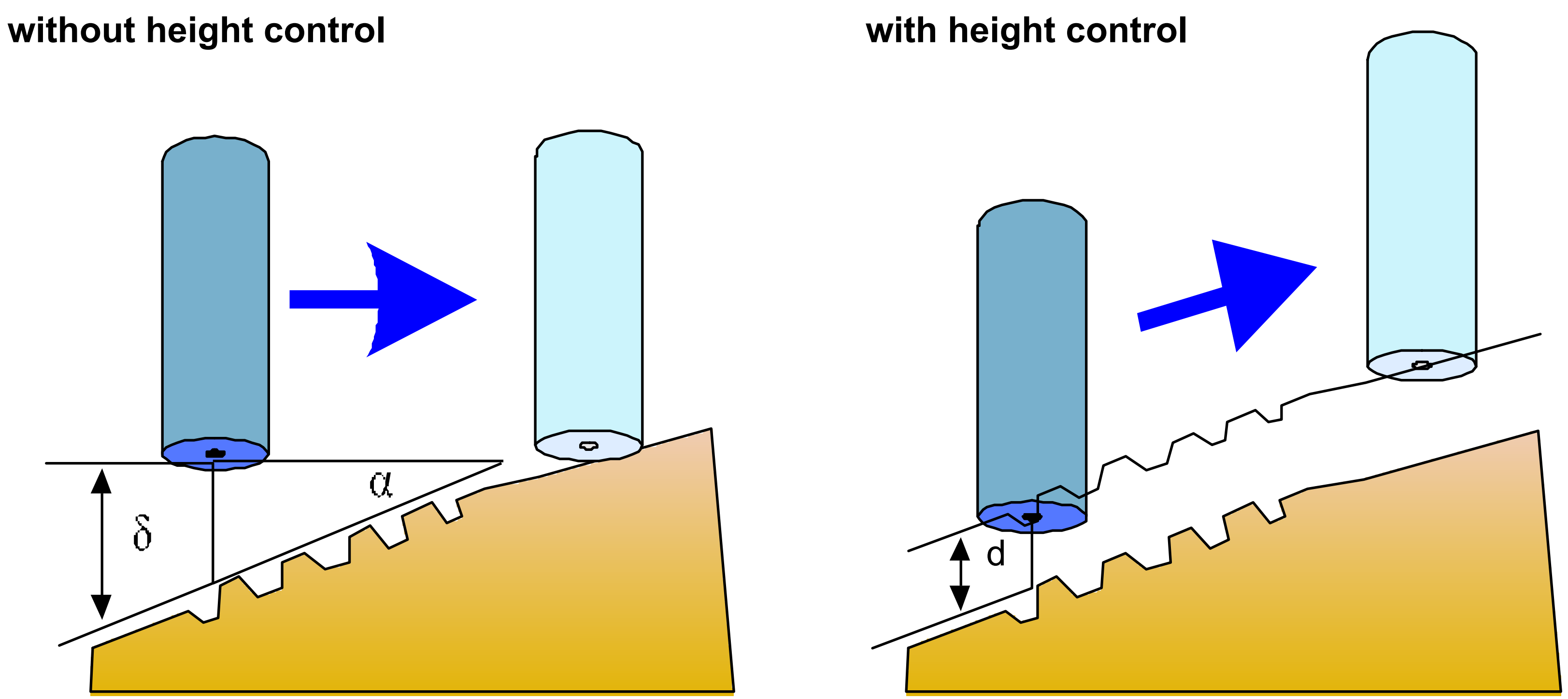

Optical shearforce mode

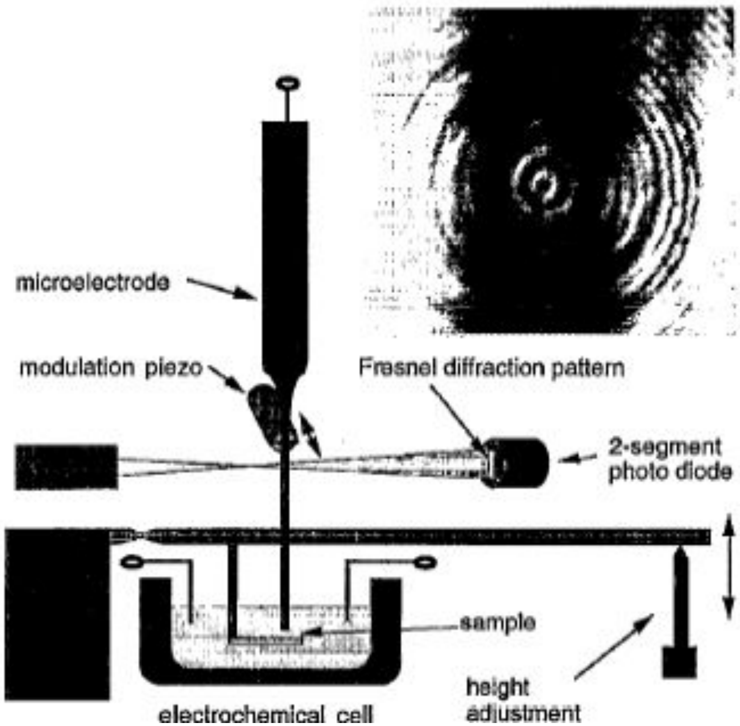

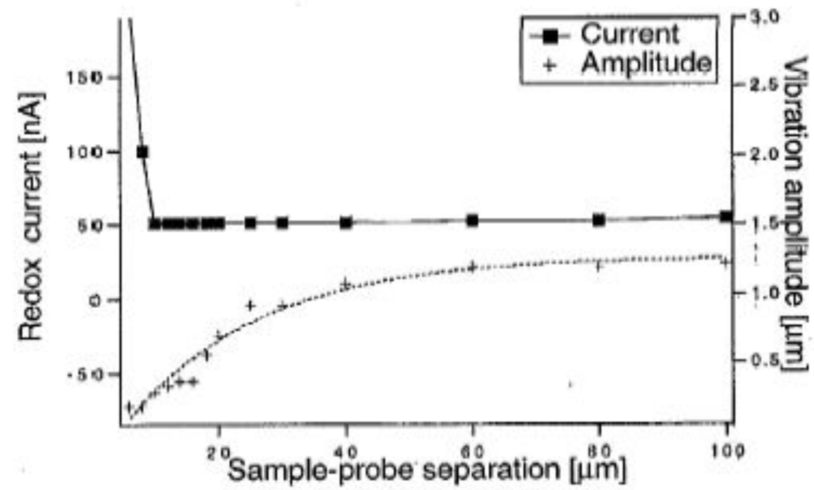

FIG. 5. Vibration amplitude and redox current as a function of the relative distance between sample holder and tip holder. The sample was a gold film on mica.

M. Ludwig, C. Kranz, W. Schuhmann, H. Gaub *Rev. Sci. Instr.* **66** (1995), 2857 *Topography feed-back mechanism for the scanning electrochemical microscope based on hydrodynamic forces between tip and sample*

Scanning Electrochemical Microscopy - High-Resolution Shearforce Positioning

Lock-In	
Poti	PC
x,y,z	nano cube

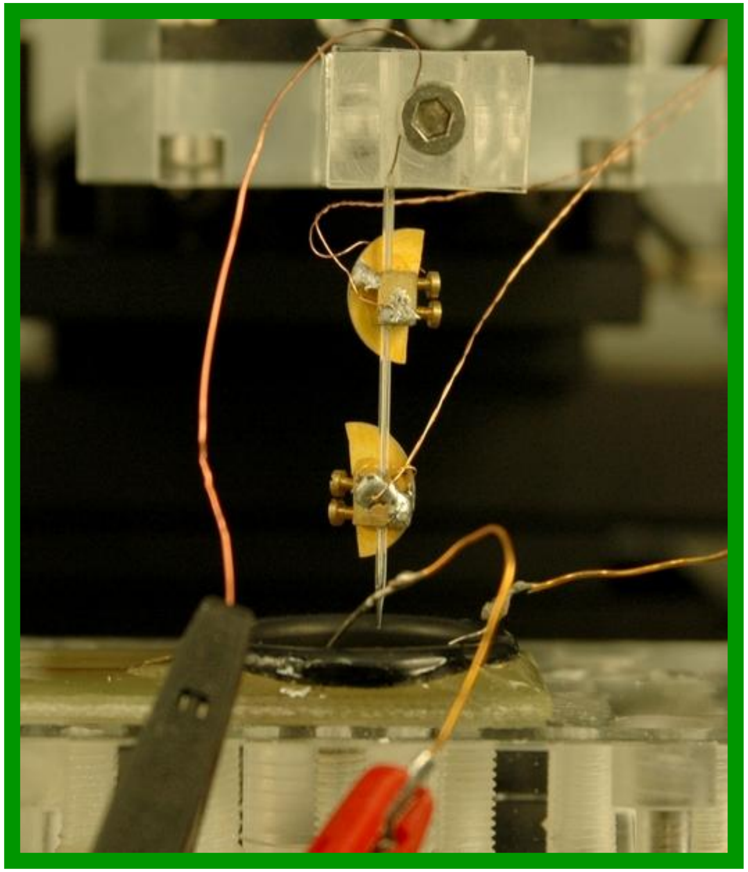

Scanning Electrochemical Microscopy – High-Resolution Shearforce Positioning

constant-height mode

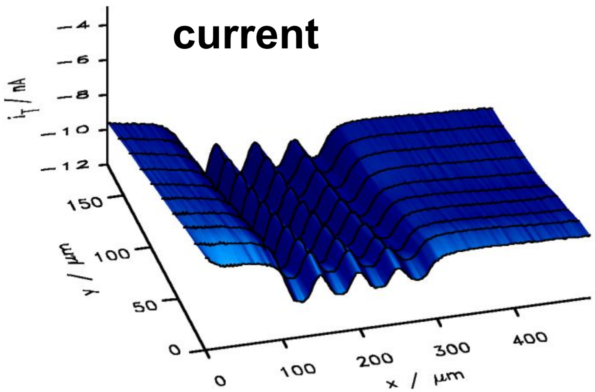

5 mM $[Ru(NH_3)_6]^{3+}$, 25 µm Pt-electrode

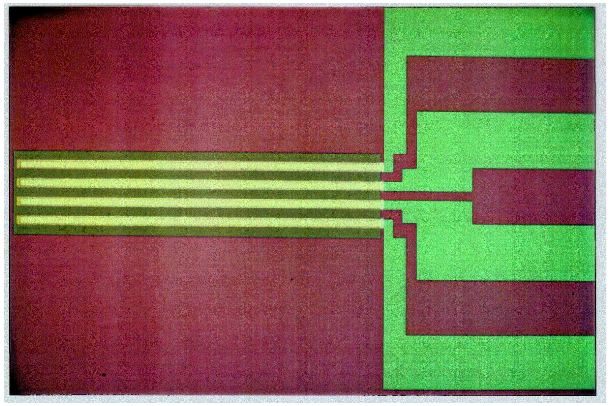

constant-distance mode

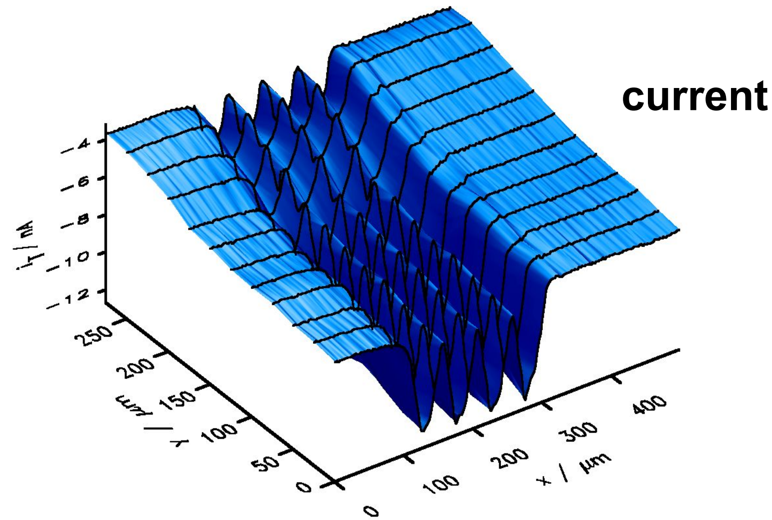

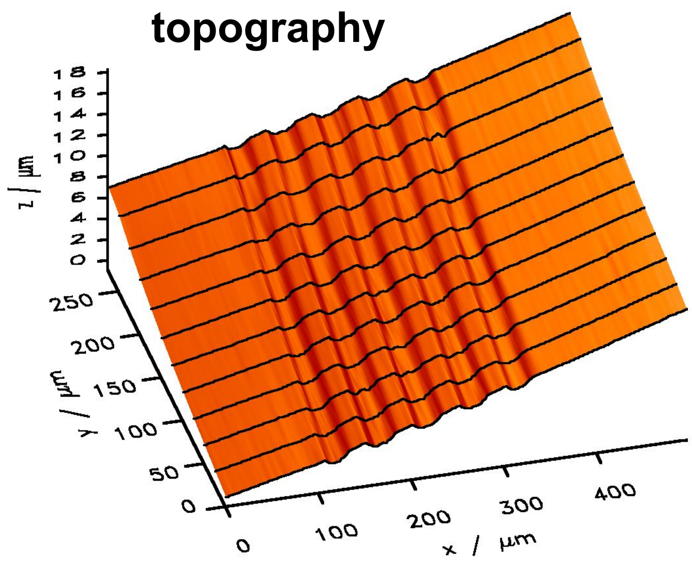

Constant-Distance Mode SECM with sub-μm Electrodes

AFM image

SECM image

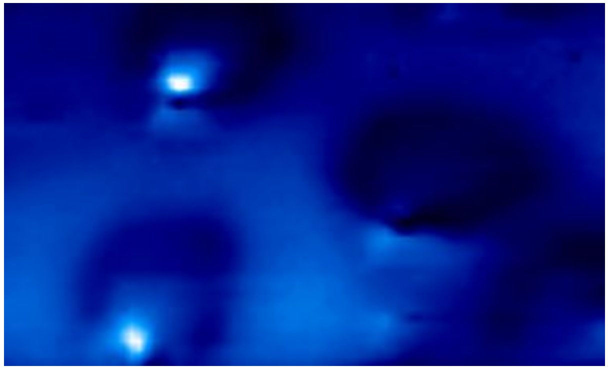

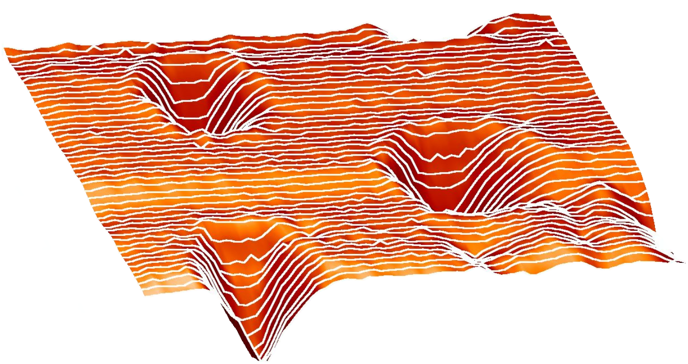

shear-force image (topography)

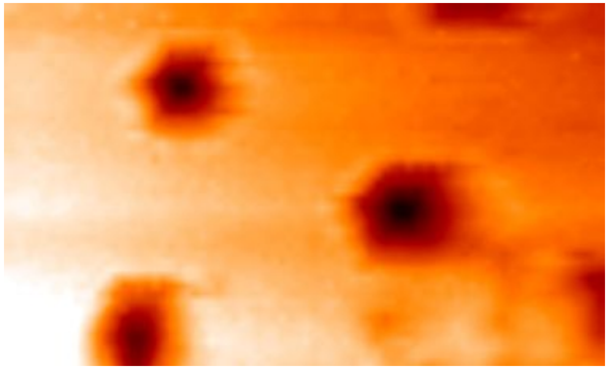

shear-force image

B. Ballesteros Katemann, A. Schulte, W. Schuhmann. *Electroanalysis* **16** (2004) 60-65. Constant-Distance Mode Scanning Electrochemical Microscopy Part II: High-resolution SECM imaging employing Pt nanoelectrodes as miniaturised scanning probes.

Hyphenated Techniques: AFM - SECM

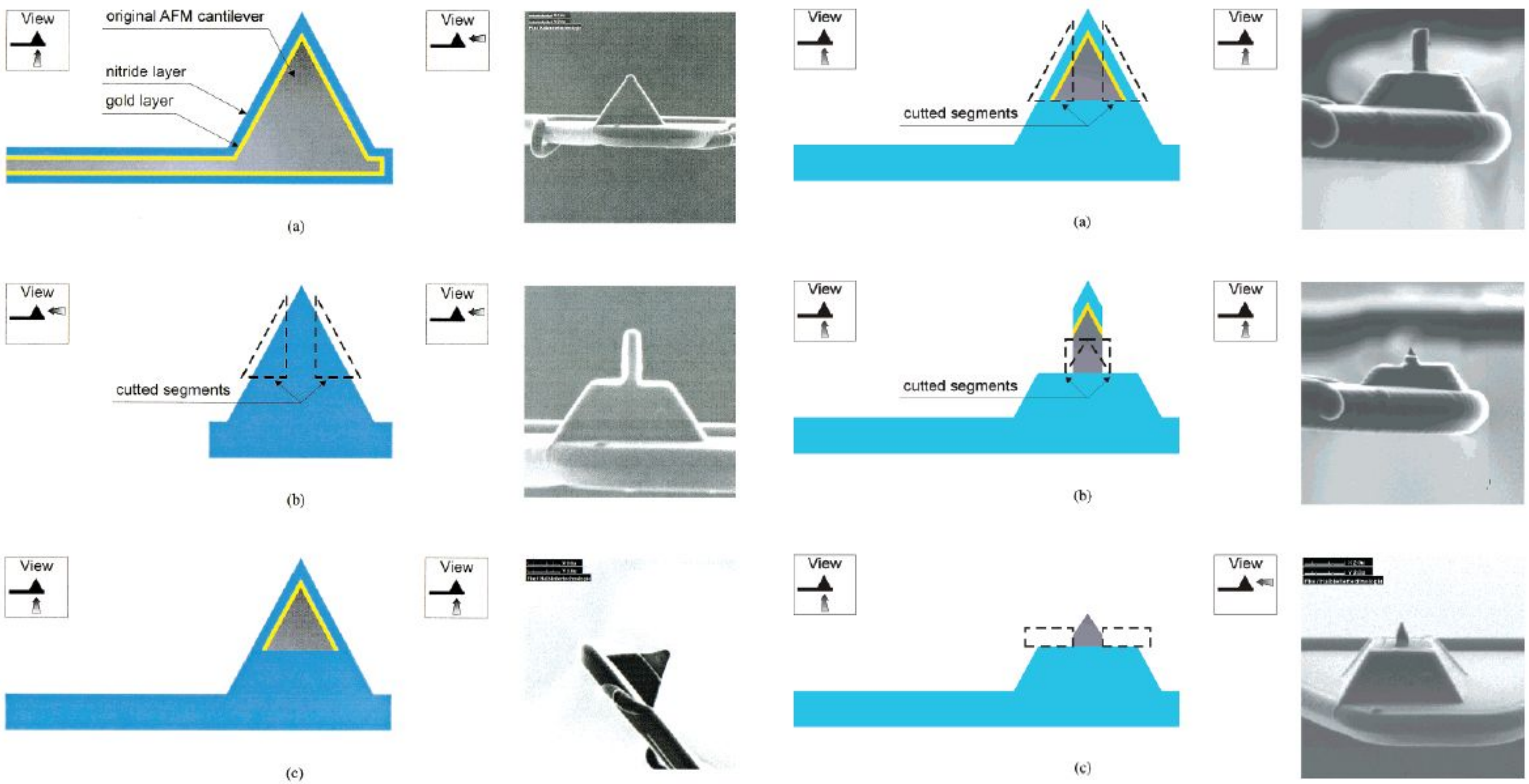

C. Kranz, G. Friedbacher, B. Mizaikoff, A. Lugstein, J. Smoliner und E. Bertagnolli, *Anal. Chem.* **73** (2001) 2491 integrating an ultramicroelectrode in an AFM cantilever: combined technology for enhanced information

Combined AFM-SECM

Bifunctional SPM probes

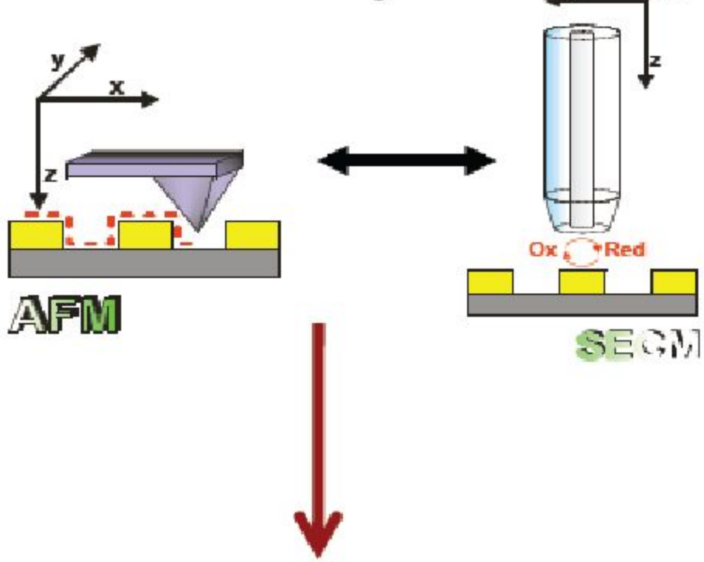

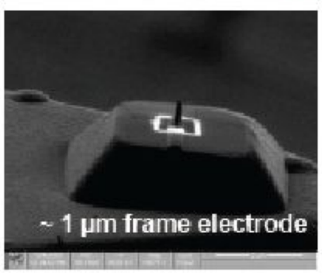

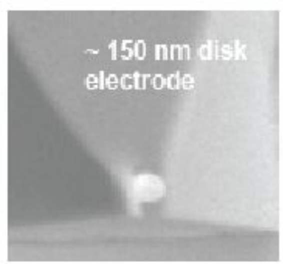

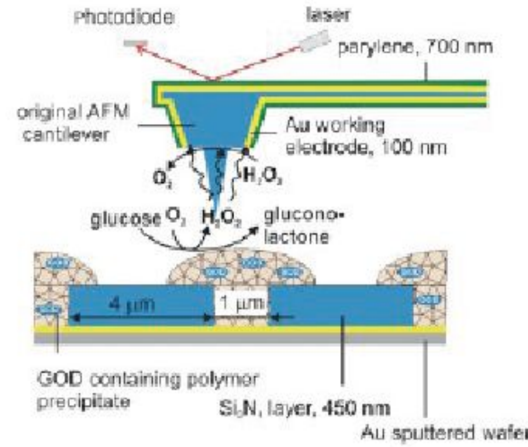

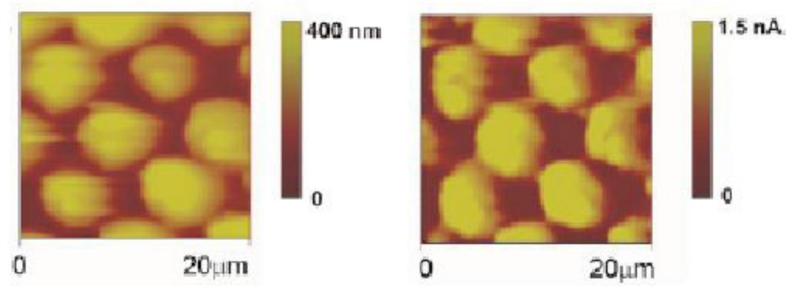

Dynamic mode images recorded in PBS (pH 7.4)
Tip-integrated electrode biased at 0.65 V vs. AgQRE

Dr. Christine Kranz
christine.kranz@uni-ulm.de